

FOR REFERENCE  
NOT TO BE TAKEN FROM THIS ROOM

MODEL ALGORITHMIC CONTROL :  
AN APPLICATION TO DC MOTOR  
SPEED CONTROL

by

Tuna ÖZPERK

BS. in EE Boğaziçi University, 1982

Submitted to the Institute For Graduate Studies in  
Science and Engineering in partial fulfillment of  
the requirements for the degree of

Master of Science

in

Electrical Engineering



Boğaziçi University

1985

MODEL ALGORITHMIC CONTROL :  
AN APPLICATION TO DC MOTOR  
SPEED CONTROL

APROVED BY

Doç. Dr. Okyay KAYNAK  
(Thesis Supervisor)

Doç. Dr. Oğuz TOSUN

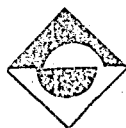
Doç. Dr. Yorgo İSTEFANOPULOS

*[Signature]*.....

*[Signature]*.....

*[Signature]*.....

DATE OF APPROVAL : 30/1/1985



## ACKNOWLEDGMENT

This thesis has been prepared for the partial fulfillment of the requirement of Bogaziçi University, School of Engineering, for the degree of Master of Science.

I wish to express my gratitude and sincere thanks to Doç. Dr. Okyay Kaynak, my thesis supervisor, for his kind interest and guidance in the accomplishment of this work. I also like to thank Sami Sarptürk for his valuable suggestions in carrying out this work.

## ABSTRACT

The growth of digital technology in the last few years has represented a challenge to automatic control research workers. The increasing use of digital minicomputers has considerably helped the industrial implementation of algorithmic types of control. For this type of control to be practical and efficient, it is imperative for the controller to have access to fast digital computing facilities with fast memory access and substantial information storage capacity.

In this thesis a new method of digital process control which is applied to a number of industrial processes ranging from power plants to glass furnaces, is described. This new control method is called Model Algorithmic Control or equivalently Model Predictive Heuristic Control. A mathematical framework for the analysis of Model Algorithmic Control is developed and the operations of the main components of the control structure are described.

The Model Algorithmic Control strategy relies on three principles:

- i. the plant is represented by its impulse response which will be used on-line by the computer for prediction,

- ii. the behavior of the closed-loop system is prescribed by means of reference trajectory initiated on the actual output,
- iii. the control variables are computed in a heuristic way. Future inputs are computed in such a way that when applied to the internal predictive model, it induces outputs as close as possible to the desired reference trajectory.

In this thesis, the Model Algorithmic Control is applied to dc motor speed control. Control algorithm is evaluated by a Z-80 based microcomputer, and the output of microcomputer is applied to a fully controlled thyristor converter unit as a speed reference input through a digital to analog converter. The actual speed of the motor is inputted to the microcomputer by means of a tachogenerator through an analog to digital converter.

The application of Model Algorithmic Control to dc motor speed control is divided in two parts. In the first part of the application, the set speed is constant, the algorithm causes the speed of the motor to reach that constant speed with a time constant similar to the reference trajectory. The time responses of motor output speed are observed for different time constants. In the second part, the set speed is time varying. In this part the set speed is changed as a linear ramp, the tracking behavior of the dc motor output speed is observed.

In chapter one, the methods for the speed control of a separately excited direct current motor are described and compared with each others. Consequently, the equations determining the dynamical behavior of the motor and the transfer function of the motor are derived.

In chapter two, solid state dc motor drives are described and the operation of a three phase full converter is explained in general terms. The features of the thyristor unit used in the realization of the control is then presented.

In chapter three, a mathematical framework for the analysis of Model Algorithmic Control is developed and the operations of the main components of the control structure are described. The equations to calculate the optimum inputs are derived.

In chapter four, the model which will be used in the algorithm is introduced. The discrete impuls response of the system is found and the overall set up for closed-loop control is given. Additionally the software developed is presented and explained.

In chapter five, the stability analysis of the Model Algorithmic Control is developed. The robustness of the system to the parameter changes is discussed. Finally the effects of the constraints on input sequence to system stability are discussed, and the experimental results are presented.

## ÖZETÇE

Geçmiş yıllarda sayısal teknolojideki önemli gelişmeler otomatik denetim araştırmacılarına yeni ufuklar açmıştır. Mikroişlemcilerin gittikçe artan kullanılım alanları, algoritma tipi denetim yöntemlerinin endüstride uygulanmalarına olanak sağlamıştır. Bu tip bir denetim yönteminin başarılı ve verimli olabilmesi için denetimi yapan mikroişlemcinin hızlı sayısal hesaplama ve hafızayı en etkili ve hızlı bir şekilde kullanabilme yeteneğine sahip olması önkoşuldur.

Bu tez çalışmasında, güç üretici dizgelerden cam işlemciliğine varana kadar pek çok endüstri uygulamalarında başarı ile denenmiş yeni bir denetim yöntemi tartışılmıştır. Bu yeni yöntem Model Algoritmusal Denetim veya Model Tahminle Deneyimsel Denetim adı verilmiştir. Model Algoritmusal Denetim yönteminin analizi için teori formüle edilmiş, denetim yönteminin temel elemanlarının işlevleri açıklanmıştır.

Model Algoritmusal Denetim yöntemi üç temel prensibe dayanmıştır:

- i. dizge, mikroişlemci tarafından dizge çıkışının tahmininde kullanılmak üzere, dürtü tepkisi ile tanımlanmıştır,
- ii. kapalı döngü dizgenin davranışı, dizge çıkışı ile başlatılan bir referans izlence ile tanımlanır,
- iii. denetim değişkeni deneysel bir yolla hesaplanmaktadır. Gelecekteki dizge girdileri, dizge çıkışını referans izlenceyi çok yakından izlemeye zorlayacak şekilde hesaplanmaktadır.

Bu tezde Model Algoritmasal Denetim yöntemi bir doğru akım motorunun hız denetimine uygulanmıştır. Denetim algoritması Z-80 tabanlı bir mikroişlemci tarafından uygulanmakta, mikroişlemci çıkışı bir sayısal analog çevirici ile tam denetimli bir tristör doğrultucunun hız referans girişine uygulanmaktadır. Motorun ansal hızı ise mikroişlemci tarafından bir analog sayısal çevirici yardımı ile takojeneratör çıkışının okunması ile elde edilir.

Model Algoritmasal Denetim bu uygulaması iki bölümde gerçekleştirilmiştir. Birinci bölümde ulaşılabilecek hız sabittir ve algoritma motor hızını bu sabit hıza, referans izlencenin zaman sabiti ile aynı olacak şekilde, ulaştıracak biçimde çalışır. Motor hızının zaman tepkisi değişik izlence zaman sabitleri için gözlemlenir. İkinci bölümde ise ulaşılabilecek hız zamanla değişkendir. Bu uygulamada ulaşılabilecek hız bir yokuş olarak alınmış ve motor hızının bu yokuş işlevini takip edişi gözlemlenmiştir.

Tezin birinci bölümünde alan uyarımlı doğru akım motorunun hız denetim yöntemleri tartışılmış, motorun dinamik davranışı incelenmiş, ve geçiş işlevi çıkarılmıştır.



İkinci bölümde katı hal doğru akım motor sürücüleri tanıtılmış ve genel olarak üç evreli tam denetimli doğrultucunun çalışması açıklanmış, ayrıca tezin uygulanmasında kullanılan tristör ünitesi tanıtılmıştır.

Üçüncü bölümde ise Model Algoritmatal Denetim yönteminin analizi için gerekli matematik çalışma yapılmış, temel denetim elemanlarının işlevlerine açıklık getirilmiş ve optimum dizge girişlerinin hesaplanması tartışılmıştır.

Dördüncü bölümde, doğru akım motorunun matematiksel modeli elde edilmiş, bu model kesikli dürtü tepkesinin bulunmasında kullanılmıştır.

Son olarak, dizgenin kararlılığı ve parametrelerdeki sapmalara karşı duyarlılığı tartışılmıştır. Ayrıca dizge girişindeki kısıtlamaların kararlılığa etkileri açıklanmıştır.

## TABLE OF CONTENTS

	page
ACKNOWLEDGMENT .....	iii
ABSTRACT .....	iv
ÖZETÇE .....	vii
LIST OF FIGURERS .....	xii
LIST OF SYMBOLS .....	xiii
I. (DIRECT CURRENT MOTOR CHARACTERISTICS)	1
A.Speed Control of Sep. Exc. DC Motor .....	2
B.Dynamics of Sep. Exc. DC Motor .....	4
C.Closed-Loop Speed Control .....	8
II. (SOLID STATE DC MOTOR DRIVES)	11
A.Phase-Controlled DC Drives .....	12
B.Three Phase Full-Converter Operation .....	13
C.Thyristor Unit Used in the Thesis .....	16
III. (MODEL ALGORITHMIC CONTROL)	25
A.Representation and Prediction .....	26
B.The Reference Trajectory .....	28
C.Optimality Criterion and the Optimal Control Strategy .....	28
D.Open-Loop and Closed-Loop Prediction .....	30
E.Tracking Type Model Algorithmic Control .....	34
IV. (MICROCOMPUTER BASED CONTROL)	36
A.Internal Model of the System .....	36
B.Software .....	43
V. (STABILITY AND EXPERIMENTAL RESULTS)	46
A.Stability .....	46

	page
1. Robustness of the System .....	49
2. Amplitude Constraints on Input .....	51
B. Experimental Results .....	53
VI. (CONCLUSIONS AND SUGGESTIONS FOR FURTHER WORK)	60
APPENDIX A :SOFTWARE OF MODEL ALGORITHMIC CONTROL FOR CONSTANT SET SPEED .....	62
APPENDIX B :SOFTWARE OF MODEL ALGORITHMIC CONTROL FOR TIME VARYING SET SPEED .....	71
BIBLIOGRAPHY .....	74

## LIST OF FIGURES

	page
FIGURE 1.1 Equivalent circuit of a sep. exc. dc motor.....	2
FIGURE 1.2 Speed control range of sep. exc. dc motor under armature voltage and field control.....	4
FIGURE 1.3 Development of motor transfer function .....	6
FIGURE 1.4 Simplified transfer function as a block diagram	7
FIGURE 1.5 Closed-loop speed control .....	8
FIGURE 2.1 Three phase full-converter .....	13
FIGURE 2.2 Three phase full-converter waveforms at diffe- rent firing angels for continuous motor current	14
FIGURE 2.3 Voltage-firing angle characteristic of full- wave converter .....	16
FIGURE 2.4 Firing pulse generating circuitry .....	21
FIGURE 2.5 Signal waveforms in the firing pulse unit .....	22
FIGURE 2.6 Three phase firing unit .....	23
FIGURE 3.1 Optimal control strategy .....	30
FIGURE 4.1 Time response of ac motor driven by thyristor unit .....	39
FIGURE 4.2 System with zero order holder .....	40
FIGURE 4.3 The grouping of coefficients in control equation	42
FIGURE 4.4 Dc motor control system .....	43
FIGURE 4.5 Flow-chart .....	44
FIGURE 5.1 Closed-loop prediction .....	48
FIGURE 5.2 Time response of the motor speed for $\alpha=0.967$	56
FIGURE 5.3 Time response of the motor speed for $\alpha=0.99$	57
FIGURE 5.4 The tracking behavior of the motor speed .....	58
FIGURE 5.5 The behavior of the system under load .....	59

## LIST OF SYMBOLS

$B$	Friction coefficient
$e_a$	Motor armature voltage
$e_g$	Motor generated voltage
$i_a$	Motor current
$J$	Moment of inertia
$K_a, K_t$	Dc machine constants
$K_s$	Speed controller gain
$K_t$	Tachogenerator gain
$L_a$	Motor armature circuit inductance
$N$	Average motor speed
$R_a$	Motor armature circuit resistance
$T$	Torque
$T_L$	Load torque
$\omega$	Angular frequency
$\phi$	Flux

## 1. DIRECT CURRENT MOTOR CHARACTERISTICS

The direct current (dc) motor is one of the first machines devised to convert electrical power into mechanical power. Many dc machines were built in the 1880's when dc was the principal form of electric power generation. With the advent of 50 Hz alternating current (ac) as the electric power standard, and invention of the induction motor with its lower manufacturing costs, the dc machine became less important. In recent years, the use of dc machines has become almost exclusively associated with applications where the unique characteristics of the dc motor (e.g. high starting torque for traction motor applications, high speed variation both above and below the rated speed) justify its cost.

The flexibility of the dc motor for speed control, its overload capability, and its reliability make it the dominant means of providing a controllable source of mechanical rotating power in industry. The steady-state characteristics of the motor determine how the motor can be controlled; the dynamic characteristics determine how the control system must be designed to obtain the required response.

### A. Speed Control of a Separately Excited DC Motor

The equivalent circuit of a separately excited dc motor shown in Fig. 1.1 is equal to a resistance,  $R_a$  (total armature circuit resistance) in series with a parallel combination of an inductance,  $L_a$  (total armature circuit inductance), and another resistance  $R_1$ . The resistance  $R_1$  will not be involved in calculations. When the motor rotates the armature coil move in the stator magnetic field. The induced e.m.f. appears across the armature terminals as internally generated voltage,  $e_g$ . Therefore the equivalent electric circuit of the motor is the impedance connected in series to a voltage source  $e_g$ .

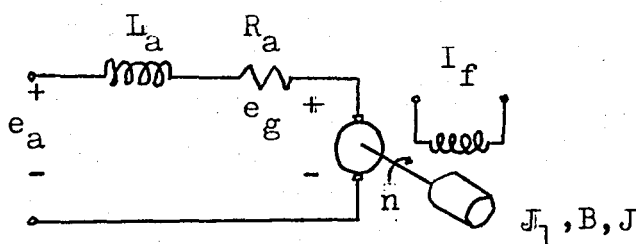


Fig. 1.1. Equivalent circuit of a sep. exc. dc motor.

The physical explanation for this model is that  $R_1$  represents the losses in the magnetic circuit. The resistance  $R_1$  is usually larger than  $R_a$  (typically about 5-10 times), and since the effect of  $R_1$  on the motor operation is insignificant, it is possible to ignore this resistance in most practical application.

The steady state operation of the motor is governed by three equations. The total armature circuit voltage is

$$e_a = e_g + i_a R_a \quad (1.1)$$

The generated armature voltage is given by

$$e_g = K_a \phi_f N \quad (1.2)$$

And, the internal torque is

$$T = K_t \phi_f I_a \quad (1.3)$$

The torque constant  $K_t$ , and armature voltage constant  $K_a$  are equal in a consistent set of units. The solution of above three equations for speed gives

$$N = \frac{e_a - R_a i_a}{K_a \phi_f} \quad (1.4)$$

Equation (1.4) shows that the speed of the motor can be controlled in three ways by changing;

- i. the armature voltage  $e_a$ , which is nearly proportional to speed
- ii. the magnetik field  $\phi_f$ , which is inversly proportional to speed
- iii. the armature circuit resistance  $R_a$ , which is proportional to the speed drop.

The control of speed by the armature circuit voltage  $e_a$  abbreviated to armature voltage control, is the most desirable because the magnetic field can remain at full amplitude and full torque can be developed. Field control is accomplished by reducing the field current and is used to extend the speed above the value for full armature voltage. In this case the available torque decreases. Armature circuit resistance control is not practical except in very small motors because of the power dissipation.



The characteristics for a full range of speed are shown in Fig. 1.2. Armature voltage control raises the speed  $N_1$ ; field control raises it additionally to speed  $N_2$ . The available torque at rated armature current is maximum to speed  $N_1$  and drops with the field to speed  $N_2$ . The horse power increases linearly to speed  $N_1$  and remains constant to speed  $N_2$ .

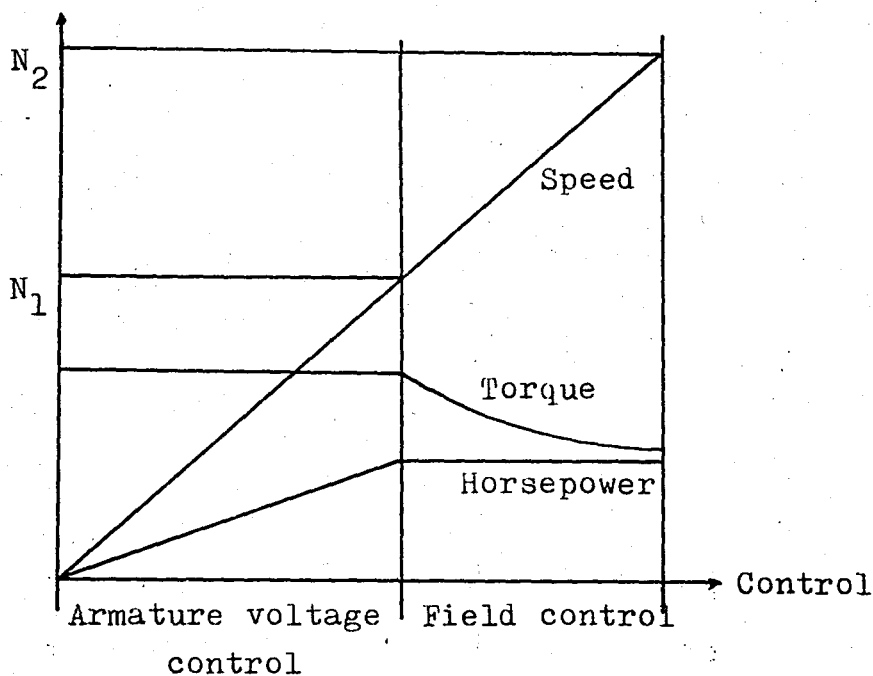


Fig. 1.2 Speed control range of sep.exc. motor under armature voltage and field control

### B. Dynamics of a Separately Excited DC Motor

The dynamic behavior of the motor is governed by its energy storage properties. Energy is stored in two places: the magnetic fields in the magnetic circuit and by mechanical velocity in the inertia of the armature. Of course, energy is also stored in the inertia of the load and in magnetic fields of the electrical sources and must be included in the consideration of the dynamics.

Consider a separately excited dc motor with armature voltage control as shown in Fig. 1.1. The voltage loop equation is

$$e_a = e_g + R_a i_a + L_a \frac{di_a}{dt} \quad (1.5)$$

where

$$e_g = K_a \phi_f n \quad (1.6)$$

The torque balance equation is

$$T_e = T_L + Bn + J \frac{dn}{dt} \quad (1.7)$$

where

$$T_e = K_a \phi_f i_a \quad (1.8)$$

In the Laplace domain, equations (1.5) through (1.8) can be written as

$$E_a(s) = E_g(s) + R_a I_a(s) + L_a s I_a(s) \quad (1.9)$$

$$E_g(s) = K_a \phi_f N(s) \quad (1.10)$$

$$T_e(s) = T_L(s) + BN(s) + JsN(s) \quad (1.11)$$

$$T_e(s) = K_a \phi_f I_a(s) \quad (1.12)$$

From equation (1.9)

$$I_a(s) = \frac{E_a(s) - E_g(s)}{R_a + sL_a} = \frac{(E_a(s) - E_g(s))/R_a}{1 + T_a s} \quad (1.13)$$

where  $T_a = L_a/R_a$  is electrical time constant of the motor armature circuit.

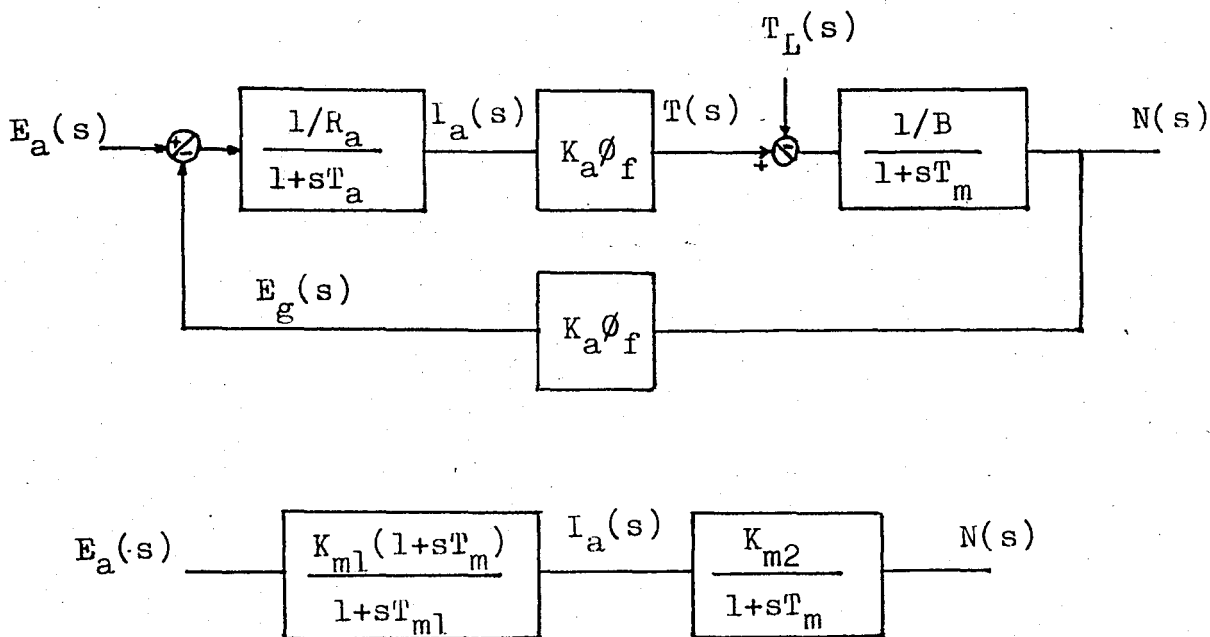


Fig. 1.3 Development of motor transfer function  
 (a). Functional block diagram  
 (b). Simplified transfer function

From equation (1.11)

$$N(s) = \frac{(T_e(s) - T_L(s))/B}{1 + T_m s} \quad (1.14)$$

where  $T_m = J/B$  is mechanical time constant of the motor.

These relationships are shown in block diagram in Fig. 1.3. The feedback loop present in the form of the back e.m.f. This back e.m.f. provides the moderate speed regulation inherent in the separately excited dc motor.

Neglecting the load torque, the relation between the speed and armature voltage is found to be

$$\frac{N(s)}{E_a(s)} = \frac{K_a \phi_f}{(K_a \phi_f)^2 + R_a B (1+sT_a)(1+sT_m)} \quad (1.15)$$

Electrical time constant  $T_a$  is always less than the mechanical time constant  $T_m$ , then  $T_a$  can be neglected and the expression simplifies to

$$\frac{N(s)}{E_a(s)} = \frac{K_a \phi_f}{(K_a \phi_f)^2 + R_a B + sR_a B T_m} = \frac{K_m}{1 + sT_{ml}} \quad (1.16)$$

where

$$T_{ml} = \frac{R_a B}{(K_a \phi_f)^2 + R_a B} T_m \quad (1.17)$$

$$K_m = \frac{K_a \phi_f}{(K_a \phi_f)^2 + R_a B} \quad (1.18)$$

Thus the motor can be represented, for the purpose of analysing it for voltage control, as a first order system as in Fig. 1.4

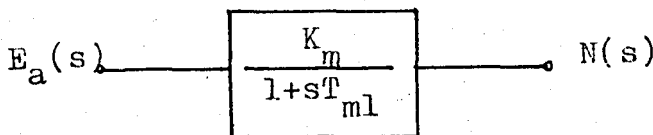


Fig. 1.4 Simplified transfer function as a block diagram

### C. Closed Loop Speed Control

If a tachogenerator is attached to the motor shaft, a speed signal which is proportional to the actual one can be fed back and the error  $E_n(s)$  used to control the armature voltage. This closed loop control scheme is shown in Fig.1.5.

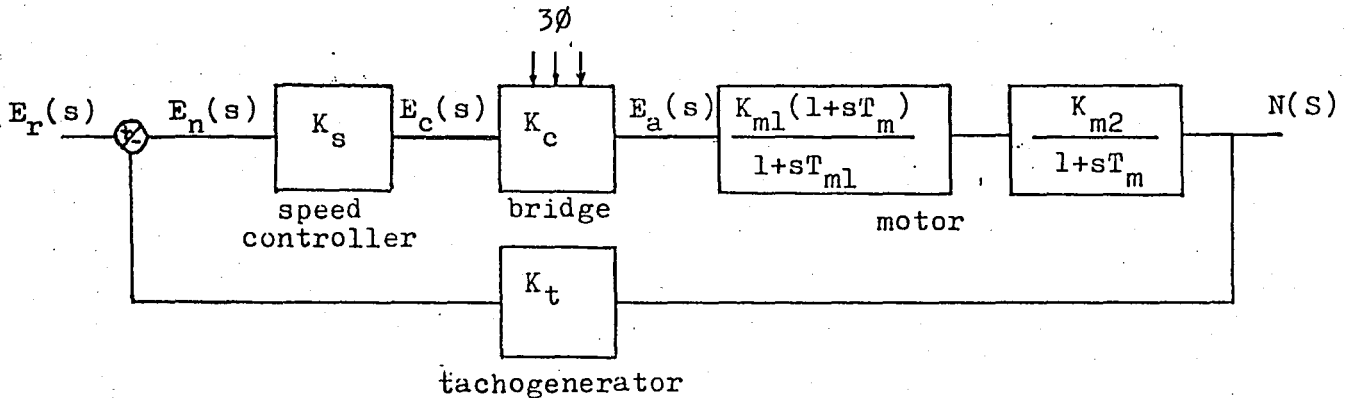


Fig. 1.5 Closed-loop Speed Control

From the block diagram shown in Fig. 1.5, the relation between the actual speed and the error is found to be

$$\frac{N(s)}{E_r(s)} = \frac{K_1}{1 + sT_1} \quad (1.19)$$

where

$$K_1 = \frac{K_s K_c K_{m1} K_{m2}}{K_s K_c K_{m1} K_{m2} K_t + 1} \quad (1.20)$$

$$T_1 = \frac{T_{m1}}{K_s K_c K_{m1} K_{m2} K_t + 1} \quad (1.21)$$

$$K_{m1} = \frac{B}{(K_a \phi_f)^2 + R_a B}, \quad K_{m2} = \frac{K_a \phi_f}{B} \quad (1.22)$$

Since  $K_s K_c K_{m1} K_{m2} K_t \gg 1$

$$K_1 = \frac{1}{K_t} \quad (1.23)$$

$$T_1 = \frac{T_{m1}}{K_s K_c K_{m1} K_{m2} K_t} \quad (1.24)$$

Also from the block diagram above

$$\frac{I_a(s)}{E_r(s)} = \frac{N(s)}{E_r(s)} \frac{I_a(s)}{N(s)} = \frac{K_1}{K_{m2}} \frac{(1+T_m s)}{(1+T_1 s)} \quad (1.25)$$

The current response to a step change in input  $E_r(s)$  is

$$I_a(s) = \frac{K_1 E_r}{K_{m2} s} \frac{(1+T_m s)}{(1+T_1 s)} \quad (1.26)$$

We can write the above equation in time domain as

$$I_a(t) = \frac{E_r K_1}{K_{m2}} \left( 1 + \frac{(T_m - T_1)}{T_1} \exp(-t/T_1) \right) \quad (1.27)$$

Since  $T_m \gg T_1$ ,  $T_1$  can be neglected. Normalizing the current with respect to the steady state  $I_a(\infty)$

$$\frac{I_a(t)}{I_a(\infty)} = 1 + \frac{T_m}{T_1} \exp(-t/T_1) \quad (1.28)$$

Therefore it can be concluded that a step input voltage results in a large sudden change in armature current which decays slowly. This transient overcurrent is undesirable from the standpoint of converter ratings and protection.

## II. SOLID STATE DC MOTOR DRIVES

Direct current (dc) motor drives are extensively used in industry all over the world. The outstanding advantages of dc drives such as ease of control, precise and continuous control of speed over a wide range and speed of response, will ensure their popularity in the future.

Thyristors (silicon-controlled rectifiers, SCRs) have revolutionized the art of speed control of drives. In the speed of variable-speed drives, a dc motor controlled by a thyristor converter is still a popular choice. In recent years, attempts have been made to develop ac drives. However, ac drives still do not compete seriously with dc drives when variable speed is required. Although ac motors are smaller in size, and require minimal maintenance, control of their speed is relatively complex and expensive. Thyristor controlled dc drives range in rating from fractional horsepower to several thousand horsepower.

The thyristor controlled dc drives have the following advantages:

- i. the thyristor-power unit eliminates the electrical time lag of the field and the armature. Time response is therefore limited only by dc motor commutating ability and the inertia of the motor,



- ii. the operation is simple and reliable,
- iii. minimal maintenance is required,
- iv. operating efficiency is high, above 95%, because of the relatively low losses in SCRs,
- v. small size, packaging flexibility, lower initial cost, and lower installation and operating costs.

The thyristor drives have the following disadvantages:

- i. the high ripple content of the converter output adds to motor heating and commutation problems. The addition of a reactor in the armature circuit may be required to smooth out the ripple current,
- ii. under certain operating conditions, the power factor in the ac supply is low,
- iii. the overload capability is low,
- iv. distortion of the ac supply voltage and telephone interference may be produced due to the switching action of SCRs,
- v. regeneration requires a complex converter control.

#### A. Phase-controlled DC Drives

In phase-controlled dc drives an ac to dc phase-controlled converter is used to control the dc drive motor. The converter changes the ac input voltage to a controllable dc output voltage. In such converters thyristor commutation is easily achieved by a process referred to as natural commutation. When an incoming thyristor is turned on, it immediately reverse biases the outgoing thyristor and turns it off. No additional circuitry is required for the commutation process. Phase-controlled converters are

therefore simple and less expensive and are extensively used in industries.

Phase-controlled converters can be classified as semi-converters and full-converters. Semi-converters are one-quadrant converters, that is, they have one polarity of voltage and current at the dc terminals. Full-converters are two-quadrant converters in which voltage polarity can reverse, but current remains unidirectional because of the unidirectional thyristors.

### B. Three Phase Full-Converter Operation

Large-horsepower dc drives take power from three phase sources. In such drives, the drive motor is controlled by three phase phase-controlled converters. The ripple frequency of the motor terminal voltage is higher than any other converters. Consequently filtering requirements for smoothing out the motor current are less. The motor current is mostly continuous, and therefore the motor performance is better than other converters.

The three phase full-converter is shown in Fig. 2.1. It uses

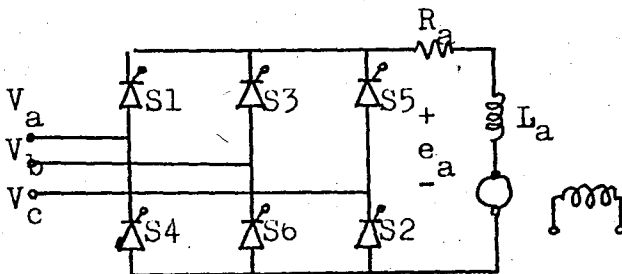


Fig. 2.1 Three phase full-converter

six thyristors and no diodes except for freewheeling operation. The thyristors are fired in sequence every  $60^\circ$  and the ripple is

always six pulses per cycle. The full wave converter produces less ripple than the three phase semi-converter, and is primarily used where regeneration is required. If the polarity of the motor armature voltage is reversed with a reversing connector or by reversing the field current, then the three phase full-converter can be operated as an inverter to transfer power from the motor to the line and finally to accelerate the motor to its required reverse speed. The voltage and current waveforms of full-converter are shown in Fig. 2.2.

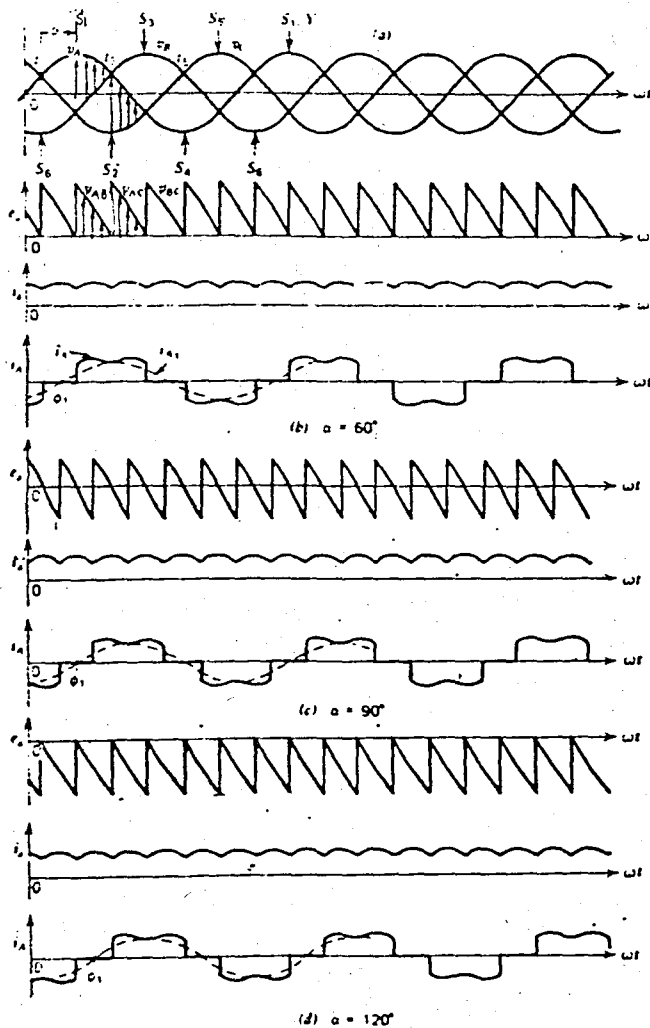


Fig.2.2 Three phase full-converter waveforms at different firing angles for continuous motor current.

At  $\omega t = \pi/6 + \alpha$ , S1 turns on. Prior to this instant S6 was turned on therefore, during the interval  $(\pi/6 + \alpha) < \omega t < (\pi/6 + \alpha + \pi/3)$ , thyristor S1 and S6 conduct, and the motor terminals are connected to phase  $V_a$  and  $V_b$ , making  $e_a = V_{ab}$ . At  $\omega t = \pi/6 + \alpha + \pi/3$ , thyristor S2 is fired, and immediately thyristor S6 is reverse biased and turns off. (Natural or line commutation) The current from S6 is transferred to S2, and therefore the motor terminals are connected to phase  $V_a$  through S1 and phase  $V_c$  through S2 making  $e_a = V_{ac}$ . This process repeats after every  $60^\circ$  whenever a thyristor is fired.

The motor terminal voltage can become negative, as shown in Fig. 2.2.d, for the triggering angle  $\alpha > 90^\circ$ . This is the inversion mode of operation of the converter.

The average motor terminal voltage can be calculated as follows: let the supply voltage be

$$\begin{aligned} V_a &= \sqrt{2} V \sin \omega t \\ V_b &= \sqrt{2} V \sin(\omega t - 2\pi/3) \\ V_c &= \sqrt{2} V \sin(\omega t - 4\pi/3) \end{aligned} \quad (2.1)$$

The average motor terminal voltage is

$$E_a(\alpha) = \frac{3}{\pi} \int_{\pi/6 + \alpha}^{\pi/6 + \alpha + \pi/3} (V_a - V_b) d(\omega t) \quad (2.2)$$

Solving the above integral one gets

$$E_a(\alpha) = \frac{3\sqrt{6}}{\pi} V \cos \alpha \quad (2.3)$$

The relation between  $E_a$  and  $\alpha$  for continuous motor current is shown in Fig. 2.3.

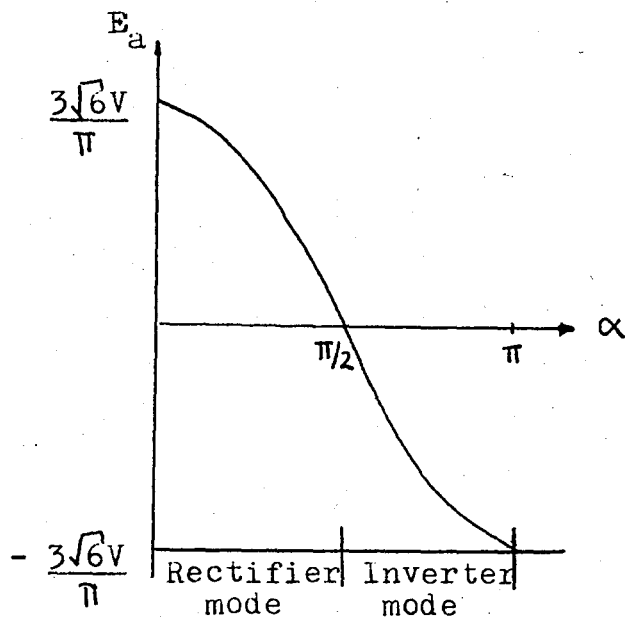


Fig. 2.3 Voltage-firing angle characteristic of full wave converter.

### C. The Thyristor Unit Used in the Thesis

In the thesis the thyristor unit CA6000 is used for the experimental work. CA 6000 is an educational three phase six pulse bridge connected, nonreversible thyristor converter which can be used for laboratory exercises or practical training.

CA 6000 is based on a modern thyristor converter "Contravas VDB 380.30", developed and manufactured for industrial applications by Contravas Antriebstechnik AG, Zurich (Switzerland) and adapted for use as a laboratory training aid. This converter in addition to all classic functional units, like speed and current controllers, firing pulse control circuits, thyristor bridge, also contains a number of auxiliary protection and monitoring functions.

which are necessary for industrial applications.

Technical specifications of Thyristor Unit CA 6000 :

Ambient temperature range	0-45° C
Rated output dc current (continuously at 45)	30 A
Input current mains side	26 A ac
Max. power dissipation	150 W
Mains frequency (selectable)	50 or 60 Hz
Mains supply voltage	3x220 or 380 V ac
Field supply dc voltage	0.9xmains supply voltage
Field current (max.)	4 A
Stabilized reference voltage	± 15 V
Speed control range (with tacho feedback)	0 - 100 % of the rated speed

The internal circuitry of the thyristor unit can be divided into two basic parts :

i. power circuitry

ii. control, protection and monitoring circuits

The power circuits basically consist of a main thyristor controlled rectifier for armature supply and an auxiliary rectifier for field excitation supply. In thyristor unit CA 6000 the main thyristor rectifier consist of a fully controlled three phase bridge connected thyristor rectifier.

The auxiliary rectifier supplies the current for the field excitation of the dc motor. In most cases, dc motors are being operated with constant field and only a simple low power single phase diode bridge like in CA 6000 is used to supply the field current.

Closed-loop automatic control circuits are used for both controlling the speed and the current of the motor. The actual speed of the motor is measured by a dc tachogenerator. This tachogenerator is a low power dc generator with permanent magnet field excitation, designed so that its output voltage is a very accurate linear function of its rotor's angular velocity. The value of actual speed and direction of rotation are thus represented by the magnitude and polarity, respectively, of the tachogenerator's output voltage.

At the input of the speed controller, the tachogenerator output (actual speed) is compared to another voltage, called speed reference, which represents the desired motor speed. The speed reference voltage can be set by means of a potentiometer inside the unit, or may come from another source. In this thesis this reference voltage is generated by the microcomputer, applying the model algorithmic control algorithm, through a digital to analog converter.

The speed reference can be fed to the speed controller's input directly or via a linear ramp. The linear ramp prevents sudden changes of the speed reference. Linear ramp limits the rate of change of speed reference to a certain, pre-settable, maximal value. The difference between the speed reference and actual speed voltages in the speed controller is thus a measure of the speed error, which has to be corrected by the control algorithm. In most drive applications, this correction has to be made as fast as possible. To determine the necessary change of the value of the armature current and to actuate this change

the following control scheme is used : Speed controller, the input signal of which is the speed error, determines the value of the current necessary to correct (or maintain) the speed, that is, the output voltage of the speed controller is the measure of the desired armature current, the current reference. A current controller then compares the signal representing the actual value of the armature current with the current reference and determines the angle at which the thyristors in the main rectifier are fired, as that the desired value of the armature current will be achieved (and maintained) ,irrispectively of the motor speed, within a short time.

The task of generating firing pulses at time instants, determined by the current controller and distributing them in the right sequence to the thyristors is performed by the firing pulse unit. The firing pulse generating circuitry is shown in Fig. 2.4. This figure actually shows only generation of firing pulses for the thyristor pair S1 and S4. Identical circuits are used for generating firing pulses for the two remaining thyristor pairs. The signal waveforms of firing pulse circuitry is shown in Fig.2.5.

The transformer  $T_r$  is used for synchronization, on the secondary part of the  $T_r$  we obtain the synchronization voltage  $U_{RT}$ . This synchronization is phase delayed by  $60^\circ$  in the RC filter (  $R_f$ ,  $C_f$  ). The zero crossing of this delayed voltage is thus coincide with the points of natural commutations of the thyristors S1 and S4. These zero crossings are detected by the zero crossing detector. Zero-crossing signal drives the saw-tooth waveform generator of which output frequency is twice the line frequency



and synchronized with the points of natural commutation of thyristors.

This saw-tooth voltage is then in the comparator compared to the control voltage  $v\alpha$  which is proportional to the firing angle. The control voltage changes from approximately 8 V in the beginning to approximately 1 V at the end, so the firing angle varies from approximately  $30^\circ$  to  $150^\circ$ .

The complete circuit for the three phase firing circuit is shown as a block diagram in Fig. 2.6.

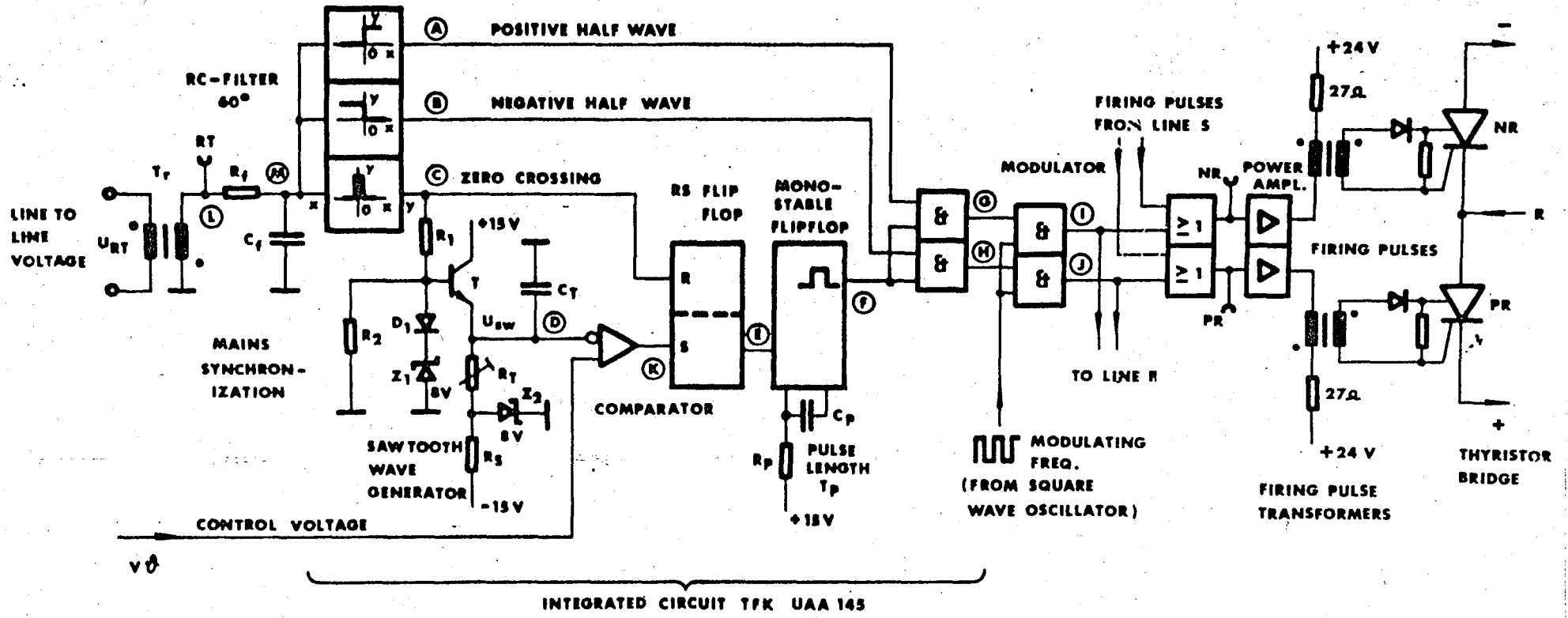


Fig. 2.4 Firing pulse generating circuitry.

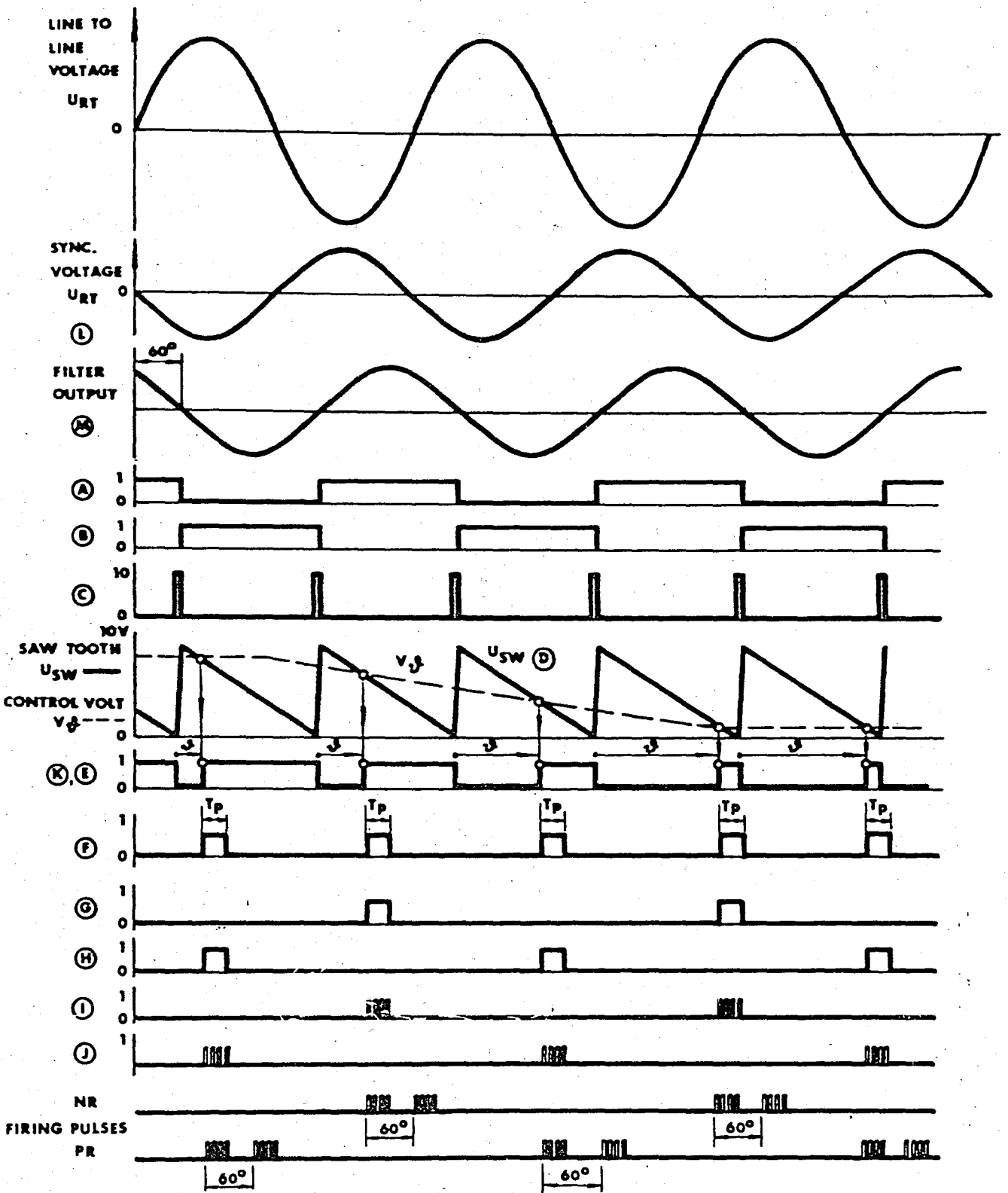


Fig. 2.5 Signal waveforms in the firing pulse unit

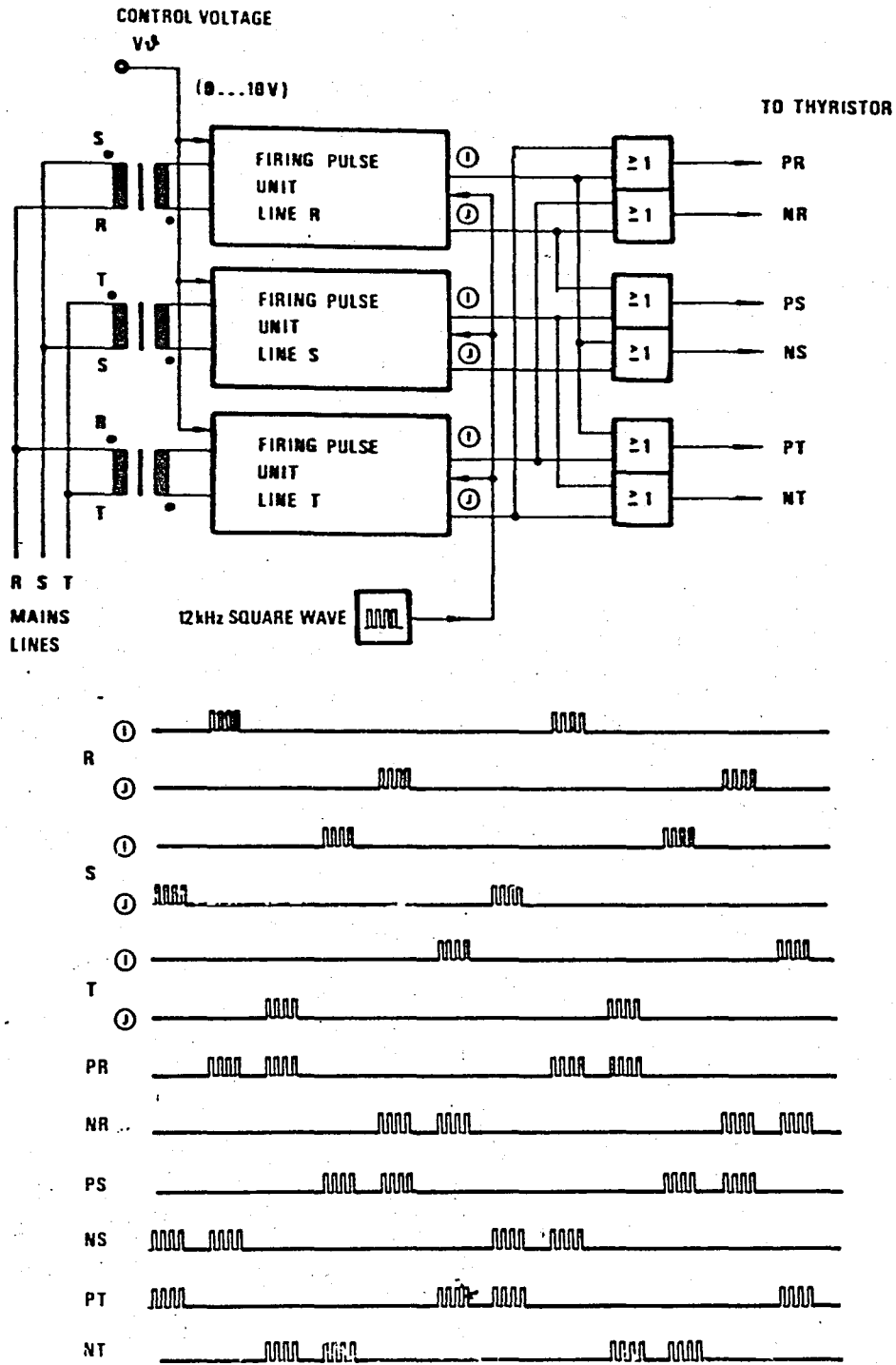


Fig. 2.6 Three phase firing unit

The speed controller part can be operated as proportional, proportional-integrating, or proportional-integrating-derivating

control by means of selectable external connections. Current control part can be operated also proportional and proportional-integrating control. In the thesis, the speed controller is achieved as proportional control.

### III. MODEL ALGORITHMIC CONTROL

The increasing use of digital microcomputers has considerably helped the industrial implementation of algorithmic-adaptive types of control. Fast digital computing facilities with fast memory access and substantial information storage capacity made the algorithmic-adaptive types of control to be practical and efficient.

The success of model algorithmic control scheme operating on a process is due to the particular representation of the process that it uses, namely impulse response representation from input to output. For most multivariable industrial processes, parametric models, such as state-space models based on physical laws are difficult to obtain. It is known that parametric models can give results with large error if the order of the model does not agree with the order of the plant. Moreover in an industrial environment, perturbations affect the plant structure more often than the measurable variables. This requires a constant checking and updating of the model parameters. The impulse response representation is convenient, since in most industrial multivariable processes, the identification of impulse response is relatively simple. The error due to truncations and approximations

of impulse responses can be looked at as a mismatch between the plant and its model. This mismatch is, partially, responsible for the discrepancy between the process output and its predicted value. The closed loop model algorithmic control, where this discrepancy enters the computation of the plant input, displays a particularly high degree of robustness against model -plant mismatch.

The model algorithmic control strategy relies on three principles :

- i. The process to be controlled is represented by its impulse response which constitute the internal model. This model is used on-line for prediction, its inputs and outputs are updated according to the actual state of the process. Though it could be identified on-line, this model is most of the time computed off-line.
- ii. The strategy is fixed by means of a reference trajectory which defines the closed-loop behavior of the plant. This trajectory is initiated on the actual output of the process and tends to the desired set-point.
- iii. Controls are not computed by a one-shot operator or controller but through a procedure which is heuristic in the general case. Future inputs are computed in such a way that, when applied to the fast time internal predictive model, they induce outputs as close as possible to the desired reference trajectory.

#### A. Representation and Prediction

The system is represented by its impulse response, the iden-

tification of which can be done both on-line and off-line. However in most cases, the off-line identification is accurate enough for the purpose of control and one can avoid the cost and complexity of an on-line identification procedure. This is due to the particular redundancy of the impulse response representation which allows a considerable enhancement of the robustness of the control scheme against identification errors and parameter perturbations.

The representation of the system is as follows :

$$y(t+1) = \underline{h}^T \underline{x}(t) = h_0 x(t) + h_1 x(t-1) + \dots + h_N x(t-N) \quad (3.1)$$

where  $y(t+1)$  is the plant output at time  $t+1$ ,  $\underline{h}^T \in \mathbb{R}^{N+1}$  denotes the plant impulse response.  $x(t-j) \in \Omega \subset \mathbb{R}$  for  $j = 0, \dots, N$ , is the input at time  $t-j$  to the plant.  $\Omega$  is the constrained set of the input.

The model (3.1) is also called the actual model to emphasize that  $\underline{h}^T$  represents the actual process. But since such a perfect knowledge of the plant impulse response is usually not possible, one has to use an approximation  $\hat{\underline{h}}^T$  to  $\underline{h}^T$ . The model corresponding to this latter impulse response is then

$$y_m(t+1) = \hat{\underline{h}}^T \underline{x}(t) . \quad (3.2)$$

The above model together with the past history of the plant output denoted by  $Y(t) = \{ y(\tau) \quad \tau \leq t \}$  is used to predict the future value of the output.



## B. The Reference Trajectory

The purpose of the control is to lead the output  $y(t)$  along a desired, and generally smooth, path to an ultimate set point  $c$ . Such a path is called a reference trajectory. From the last sampled value  $y(t_0)$  a trajectory  $y_r(t_0+k)$  is initialized which reaches  $c$  according to some criterion ( e.g. no overshoot, fixed time response ). The desired values of the future output can be obtained from stored data or computed by a recursive equation. One of the simplest ( first order ) reference trajectory is

$$y_r(t_0+k) = \alpha^k y_r(t_0) + (1-\alpha^k)c \quad |\alpha| < 1$$

$$y_r(t_0) = y(t_0) \quad (3.3)$$

The control algorithm has to find a set of future control variables such that the future outputs of the internal model will be as close as possible to the reference trajectory.

The reference trajectory can be chosen to be of higher order and the set point can be made time variant.

## C. The Optimality Criterion and the Optimal Control Strategy

The optimality criterion should reflect the previously mentioned purpose of following the reference path to the desired set point  $c$ . This can be done by defining the optimum control strategy as the one which minimizes over a certain horizon in the future, the deviation of the predicted outputs from the reference path.

Formally, at each instant  $t_0$ , the optimum set of  $T$  future inputs  $\{x^*(t_0), x^*(t_0+1), \dots, x^*(t_0+T-1)\}$  are such that the predicted  $T$  outputs  $\{y_p(t_0+1), \dots, y_p(t_0+T)\}$  are as close as possible, in the sense of a weighted Euclidean norm, to the reference trajectory. Therefore the function to minimize is

$$J_T = \sum_{k=1}^T (y_p(t+k) - y_r(t+k))^2 w_k \quad (3.4)$$

where  $w_k$  is a nonnegative weighting factor.

The interval  $\{t_0, t_0+T\}$  is called the horizon of control evaluation, and sometimes the horizon of prediction since at time  $t_0$  one has to predict a set of  $T$  outputs  $y_p(t+k)$ , ( $k=1, 2, \dots, T$ ). Once the set  $X^*(t_0)$  of the optimum inputs is determined, it is possible to wait up to  $T$  periods before observing the process output  $y(t)$ , and reinitializing  $y_r(t)$ , predicting  $y_p$ 's and computing the next set  $X^*(t_0+T)$ . This means that all the elements of the optimum control set  $X^*(t_0)$  have been actually applied to the plant.

In this thesis, the horizon of control evaluation is selected as a one sampling period. This is called one-step prediction. The reference trajectory for one-step prediction is continuously initialized on the observed plant outputs  $y(t_0), y(t_0+1), \dots, y(t_0+T-1)$  that is

$$y_r(t_0+j) = \alpha y(t_0+j-1) + (1-\alpha)c,$$

$$\forall j=1, \dots, T \quad (3.5)$$

Also the optimality criterion requires that

$$J_1 = (y_r(t+1) - y_p(t+1))^2 w_1 \quad (3.6)$$

$$y_r(t+1) = y_p(t+1) \quad (3.7)$$

The optimal control strategy is then, as shown schematically in the Fig. 3.1, realized as follows : At time  $t_0$ , the plant output is predicted from the reference trajectory, then the optimum input is calculated to lead the process to follow the reference trajectory as closely as possible.

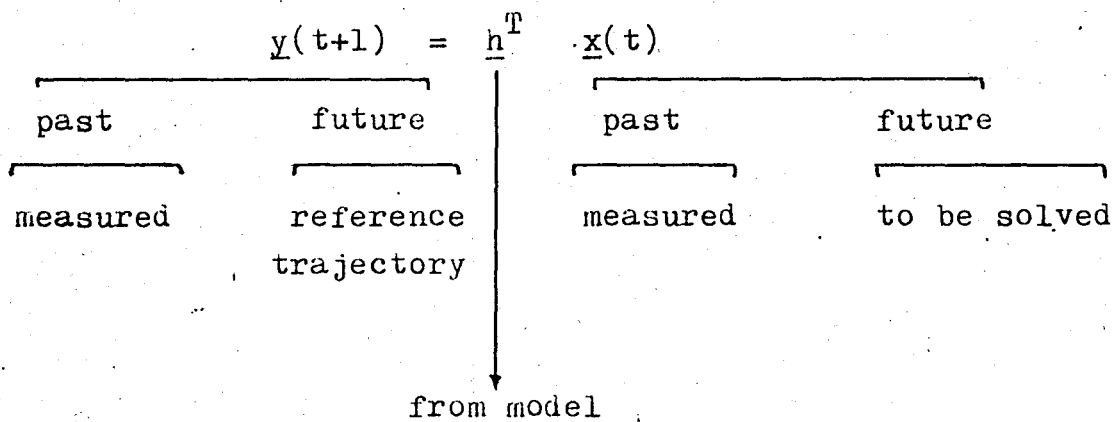


Fig. 3.1 Optimal control strategy

#### D. Open-Loop and Closed-Loop Prediction

The simplest one step ( $T=1$ ) open-loop prediction scheme that one can imagine is

$$y_p(t+1) = y_m(t+1) = \hat{h}^T x(t), \quad (3.8)$$

that is, the model of the plant is used to predict the output one step ahead. The main inconvenience of such a prediction is that the output  $y(t)$  of the controlled plant would not converge to the set point  $c$  when there is a mismatch between the model and the plant.

From equations (3.7) and (3.5)

$$y_p(t+1) = \alpha y(t) + (1-\alpha)c, \quad (3.9)$$

and writing the above equation in the expanded form, we get

$$\hat{h}_0 x(t) + \hat{h}_1 x(t-1) + \dots + \hat{h}_N x(t-N) - \alpha (h_0 x(t-1) + h_1 x(t-2) + \dots + h_N x(t-N-1)) = (1-\alpha)c \quad (3.10)$$

$$\hat{h}_0 x(t) + (\hat{h}_1 - \alpha h_0) x(t-1) + (\hat{h}_2 - \alpha h_1) x(t-2) + \dots + (\hat{h}_N - \alpha h_{N-1}) x(t-N) - \alpha h_N x(t-N-1) = (1-\alpha)c \quad (3.11)$$

If the system is stable, the sequence converges to a value  $\bar{x}$ , then

$$(\hat{h}_0 + \hat{h}_1 - \alpha h_0 + \hat{h}_2 - \alpha h_1 + \dots + \hat{h}_N - \alpha h_{N-1} - \alpha h_N) \bar{x} = (1-\alpha)c \quad (3.12)$$

Therefore

$$\bar{x} = \frac{(1 - \alpha)c}{\sum_{i=0}^N \hat{h}_i - \alpha \sum_{i=0}^N h_i} \quad (3.12)$$

The output for this input is

$$y = h^T \bar{x} = \frac{(1 - \alpha)c \sum_{i=0}^N \hat{h}_i}{\sum_{i=0}^N \hat{h}_i - \alpha \sum_{i=0}^N h_i} \quad (3.13)$$

The difference between the set point and the output is

$$y - c = \left( \frac{(1 - \alpha)c \sum_{i=0}^N \hat{h}_i}{\sum_{i=0}^N \hat{h}_i - \alpha \sum_{i=0}^N h_i} - 1 \right) c \quad (3.14)$$

Therefore the bias term is found to be

$$\frac{\sum_{i=0}^N \hat{h}_i - \sum_{i=0}^N h_i}{\sum_{i=0}^N \hat{h}_i - \alpha \sum_{i=0}^N h_i} c \quad (3.15)$$

To alleviate the bias problem, the closed-loop prediction is applied. The closed-loop prediction is as follows :

$$y_p(t+1) = y_m(t+1) + (y(t) - y_m(t)) \quad (3.16)$$

where  $y(t) - y_m(t) = (\underline{h} - \hat{\underline{h}}) \underline{x}(t-1)$  represents a correction term similar to the innovation term of Kalman filter or the correction term of an observer, assuring the final convergence of the plant output to the set point.

Rewriting the equation (3.9)

$$y_p(t+1) = y_r(t+1) = \alpha y(t) + (1-\alpha)c, \quad (3.17)$$

and inserting this equation into the equation (3.16), we get

$$(1-\alpha)(c - y(t)) = y_m(t+1) - y_m(t). \quad (3.18)$$

Assuming that the system is stable, as  $t \rightarrow \infty$  it can be shown that

$$(1 - \alpha)(c - y(t)) = 0$$

then

$$\lim_{t \rightarrow \infty} y(t) = 0 \quad (3.19)$$

The optimum sequence of inputs  $x^*(t)$  in the sense of minimizing  $J_1$ , for a closed-loop system, is generated by an auto-regressive equation, which results from equation (3.18), where  $y_p(t+1)$  and  $y_r(t+1)$  are expressed in terms of inputs

$$(1-\alpha)\left(c - \sum_{j=0}^N h_j x(t-j-1)\right) = \sum_{j=0}^N \hat{h}_j x^*(t-j) - \sum_{j=0}^N \hat{h}_j x^*(t-j-1) \quad (3.20)$$

$$(1-\alpha)\left(c-\sum_{j=0}^N h_j x(t-j-1)\right) = \hat{h}_0 x^*(t) + \sum_{j=1}^N \hat{h}_j x^*(t-j) - \sum_{j=0}^N \hat{h}_j x^*(t-j-1) \quad (3.21)$$

Therefore the optimum input is

$$\hat{h}_0 x^*(t) = \sum_{j=0}^N \hat{h}_j x^*(t-j-1) - \sum_{j=1}^N \hat{h}_j x^*(t-j) + (1-\alpha)\left(c-\sum_{j=0}^N h_j x(t-j-1)\right) \quad (3.22)$$

The summation in the last term in the equation (3.22) can be written as  $y(t)$  because this summation is the actual speed obtained by measurements at every sampling instants. Also we can write the summations in the above equation in opened form and making some manipulations we get

$$x^*(t) = \left(\frac{\hat{h}_0 - \hat{h}_1}{h_0}\right)x^*(t-1) + \left(\frac{\hat{h}_1 - \hat{h}_2}{h_0}\right)x^*(t-2) + \dots + \left(\frac{\hat{h}_N - \hat{h}_{N-1}}{h_0}\right)x^*(t-N-1) - \frac{\hat{h}_N}{h_0}x^*(t-N) + \frac{(1-\alpha)}{h_0}(c-y(t)) \quad (3.23)$$

### E. Tracking Type Model Algorithmic Control

In many applications, it is desired for the output of the system under the control to track a certain trajectory. The tracking behavior of the output does not complicate the theory of model algorithmic control. The only thing that we should have to do is to make the set point  $c$  time varying.

Time varying set speed can be achieved in different ways. For example, the desired trajectory might be the output of another

process. If at each sampling interval the computer reads this external process output as a set speed  $c$ , then the output of controlled process follows the time varying set speed, the output of the external process. The rate of change of external process output, of course, must be slower than the time constant of the software trajectory. If the time constant of software trajectory is lower than the external process, there will be always error between the desired trajectory and the process output, because the software trajectory will not have enough time to follow the external process output.

In the thesis, the time varying set speed  $C(t)$  is in the form of a linear ramp, the slope of which is made equal to desired acceleration. The maximum acceleration of the motor output can be calculated from the equation (1.7) by neglecting the load torque

$$T_e = Bn + J \frac{dn}{dt} = K_a \phi_f i_a \quad (3.24)$$

For maximum speed and maximum generated torque, maximum acceleration  $\frac{dn}{dt}$  is calculated. If the maximum speed is divided by the maximum acceleration, the time that the ramp reaches the maximum speed is found.

For the parameters of the system that the experimental investigations were carried on, the maximum acceleration that the system is capable of was found to be  $11.27 \text{ rad/sec}^2$ .



#### IV. MICROCOMPUTER BASED CONTROL

In this chapter the design of a microprocessor based control of a dc motor fed by a three phase full-converter is described. The system is realized by Z-80 based microcomputer. The microcomputer manipulates the software of model algorithmic control and communicates with the thyristor unit and the tachogenerator through a D/A converter and a A/D converter respectively.

##### A. The Internal Model of the System

The purpose of the internal model as mentioned in chapter three is to have a flexible representation of the controlled system stored in the microcomputer memory, which can be updated as the system changes and which can be used at any instant to predict the future behavior of the system under different control inputs.

The internal model of the system is generally obtained via off-line identification, using either a physical model structure when one is available or an input-output type representation model such as the impulse response model.

The simplified transfer function of the dc motor is

$$\frac{N(s)}{E_a(s)} = \frac{K_m}{1 + sT_{ml}} \quad (4.1)$$

where

$$K_m = \frac{K_a \phi_f}{(K_a \phi_f)^2 + R_a B} \quad (4.2)$$

$$T_{ml} = \frac{R_a B}{(K_a \phi_f)^2 + R_a B} T_m \quad (4.3)$$

In order to be able to identify the dc motor used in the thesis, we have to find the motor parameters  $K_a \phi_f$ ,  $B$ ,  $J$ ,  $R_a$  and  $T_m$ . These parameters are found with the help of thyristor unit, so the transfer function obtained at the end of experiments represents both the thyristor unit and the dc motor.

The armature resistance  $R_a$  is measured when the motor is hot by using an ohm-meter. This measurement is repeated for different angular positions and the average value is calculated. After this process  $R_a$  is found to be 4.8 ohms.

The back e.m.f. constant  $K_a \phi_f$  is obtained by running the machine as a generator at the rated field current and calculating the ratio of the generated voltage to speed.  $K_a \phi_f$  is found to be 1.361 V/rad/sec.

The mechanical damping coefficient  $B$  is found with the help of equation below

$$J \frac{d\omega}{dt} + B\omega + T_L = T_e = K_a \phi_f I_a \quad (4.4)$$

If the machine rotates at a constant speed and no load is applied the equation (4.4) reduces to

$$B\omega = K_a \phi_f I_a \quad (4.5)$$

Measuring the  $I_a$  at rated speed, and repeating this a few times  $B$  is found to be 0.006498 rad/V.sec .

The equation (4.4) is also utilized in finding the total motor armature and tachogenerator inertia  $J$ . The speed reference potentiometer of the thyristor unit is preset to the value that the motor rotates at 1400 rpm. The start switch is depressed and by means of a storage oscilloscope the acceleration recording in Fig. 4.1 is obtained. Since no load is applied the equation (4.4) becomes

$$J \frac{d\omega}{dt} + B\omega = K_a \phi_f I_a \quad (4.6)$$

and the armature current is measured to be 0.85 A. Because of the internal dynamics of the thyristor unit, the acceleration recording consists of two parts with different time constants. Only the interval from 0 to 0.5 sec. part is considered for the calculation of  $J$ .

The slope in the interval 0 to 0.3 sec. is about  $\frac{d\omega}{dt} = \frac{5.75}{1.5}$

then

$$J \frac{5.75}{1.5} + 0.0065 \frac{1150 \cdot 2\pi}{60} = 1.361 \cdot 0.85$$

Solving the above equation the total inertia is found to be

$$J = 0.098 \text{ kg-m}^2.$$

The transfer function of the system is then

$$\frac{N(s)}{E_a(s)} = \frac{0.722}{1 + 0.249s} \quad (4.7)$$

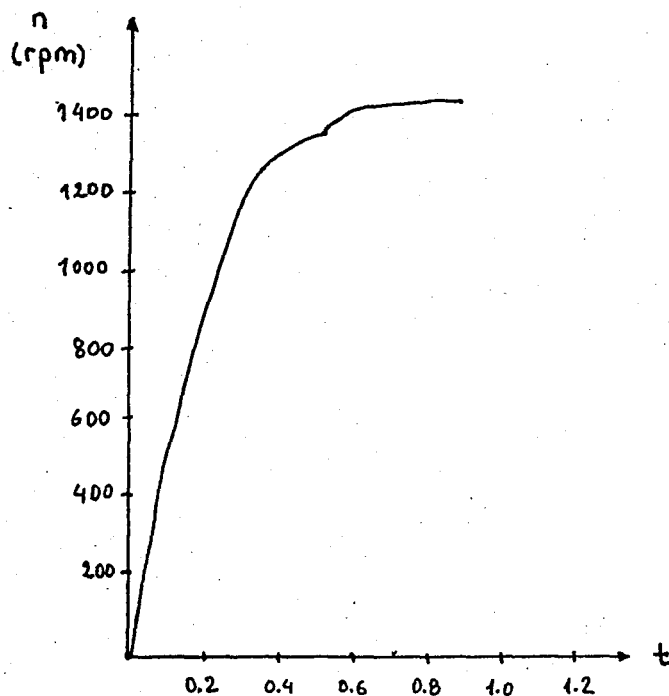


Fig. 4.1 Time response of dc motor driven by thyristor unit..

The next step is to find the discrete impulse response of the dc motor. The control input  $e_a(t)$  is assumed to be piecewise constant, then the system is as in Fig. 4.2.

$$G(s) = \frac{N(s)}{E_a(s)} = \frac{1 - e^{-sT}}{s} \cdot \frac{b}{s+a} \quad (4.8)$$

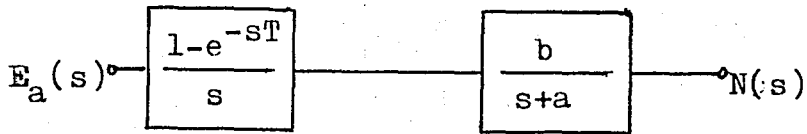


Fig. 4.2 System with Zero Order Holder

In the Z domain the equation (4.8) is

$$G(z) = z \left\{ \frac{b}{a} (1 - e^{-sT}) \left( \frac{1}{s} - \frac{1}{s+a} \right) \right\} . \quad (4.9)$$

Our system representation was  $y(t+1) = \underline{h}^T x(t)$  so the output in the Z domain is multiplied by  $z$  then the transfer function in Z domain is

$$H(z) = z G(z) \quad (4.10)$$

then

$$H(z) = \frac{b}{a} (z-1) \left( \frac{z}{z-1} - \frac{z}{z-e^{-aT}} \right) \quad (4.11)$$

$$H(z) = \frac{b}{a} (1 - e^{-aT}) \frac{z}{z-e^{-aT}} \quad (4.12)$$

The discrete impulse response is found by taking inverse Z transformation of the above equation. It is found to be

$$h(kT) = \frac{b}{a} (1 - e^{-aT}) e^{-akT} \quad \text{for } k=0,1,\dots,N \quad (4.13)$$

where  $a = 2.893$  and  $b = 4.001$ .

$N$ , which is the number of the impulses to approximate the dc motor, is selected such that the  $h_N$  can be considered as zero. The sampling period  $T$  is selected as 8 msec. This time interval limits the computer time to calculate the control inputs at every sampling period. For the system used in the thesis  $N$  is selected as 145, because time limit lets us only that amount of data to manipulate.

As it is mentioned in chapter three, for model algorithmic control to be practical and efficient, the controller must have fast digital computing facilities. Our system is controlled by a Z-80 based microcomputer with clock frequency 2.5 MHz. This clock frequency never let us to be able to manipulate 145 multiplications and the same number of summations. This limitation forces us to group the coefficients in equation (3.25), without disturbing the exponential decay of them as much as possible. This approximation is shown schematically in Fig. 4.3.

Grouping the coefficients in equation (3.25) considerably reduces the computation time of the control inputs. Instead of 145 multiplications and 145 summations the computer does 145 summations and 13 multiplications. The multiplication program consumes much more time than the summation, so reducing the number of multiplications saves quite an important amount of computation time.

Normalized  
with  
respect to  
 $h_0$

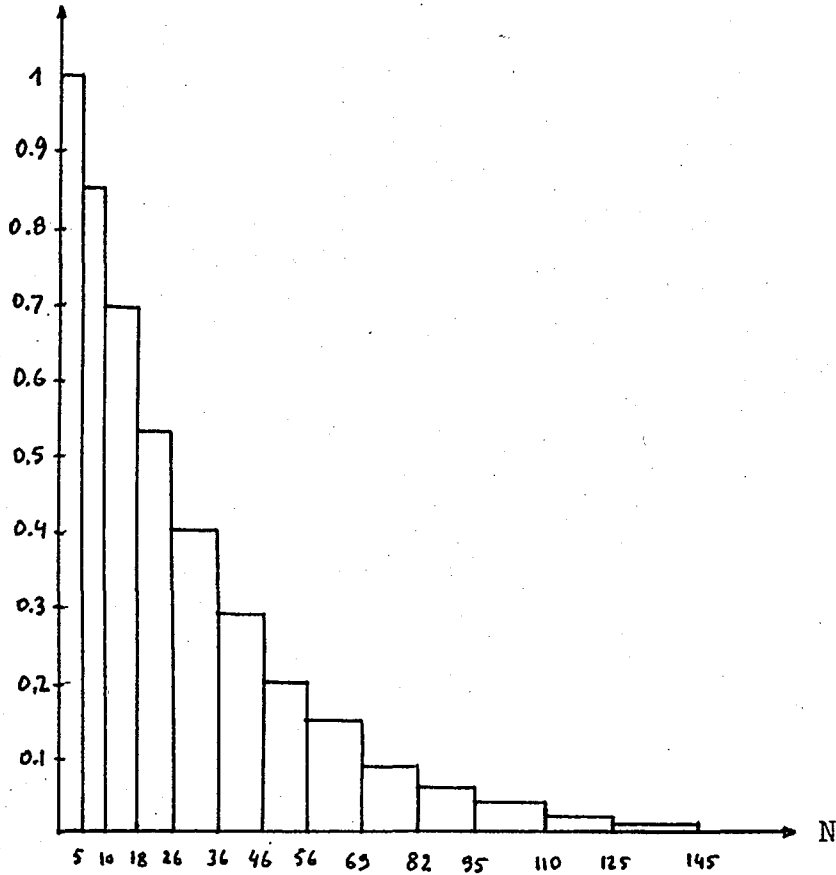


Fig. 4.3 The grouping of coefficients  
in control equation

The overall model algorithmic control system is shown  
as a block diagram in Fig. 4.4.

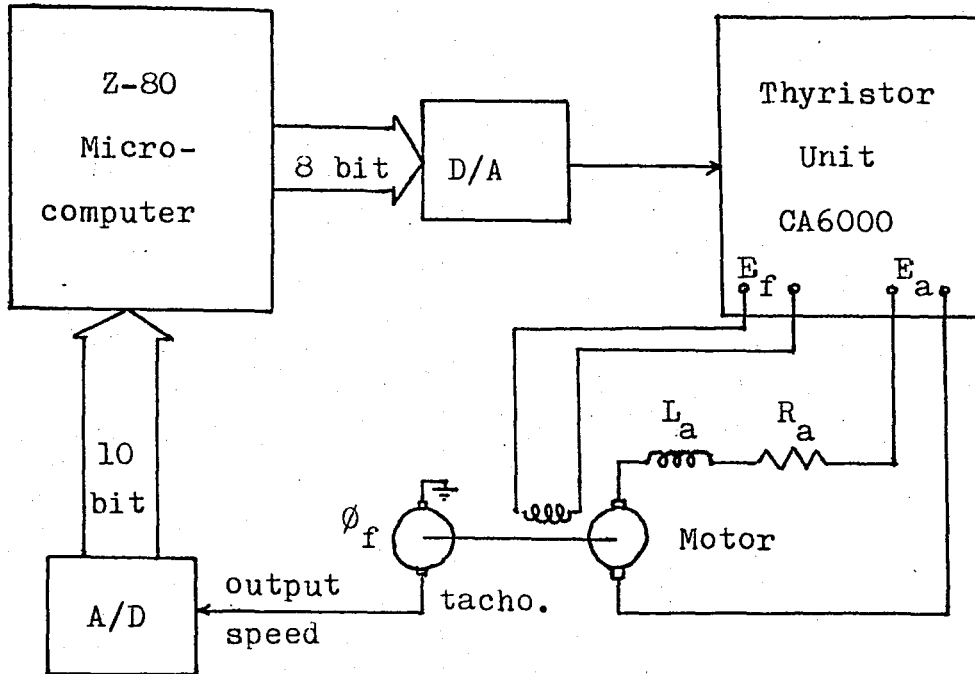


Fig. 4.4 Dc motor speed control system

## B. Software

The optimum control input  $x^*(t)$  was found in the previous chapter in equation (3.23). The coefficients in this equation are precalculated by solving the equation (4.13), discrete impulse response, and located in the memory of the microcomputer. The software of model algorithmic control for constant set speed in the memory solves the equation (3.23) for  $x^*(t)$ . The flow-



chart of the program developed is given in Fig. 4.5 and the software listing in Appendix A. Since software takes 8msec calculation time which is equal to the sampling period, an external timer is not included in the hardware of the system.

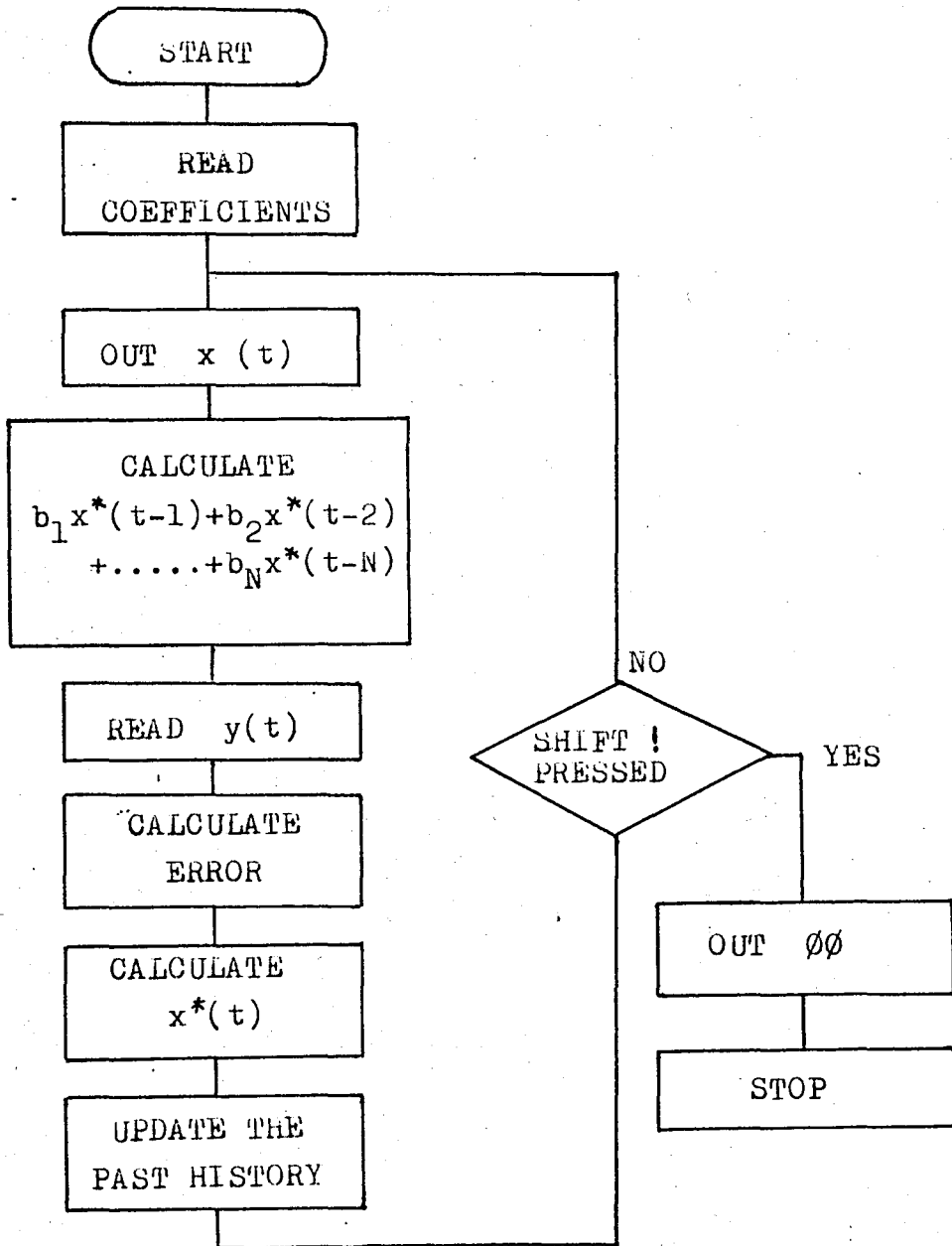


Fig. 4.5 Flow-chart

Also the software listing for model algorithmic control for time varying set speed is given in Appendix B.

## V. STABILITY AND EXPERIMENTAL RESULTS

### A. Stability

The optimum sequence of inputs  $x^*(t)$ , obtained such that the outputs minimizes  $J_1$ , for a closed-loop system, was generated in chapter 3 by an auto-regressive equation, where  $y_p(t+1)$  and  $y_r(t+1)$  are expressed in terms of inputs.

$$\hat{h}_0 x^*(t) = \sum_{j=0}^N \hat{h}_j x^*(t-j-1) - \sum_{j=1}^N \hat{h}_j x^*(t-j) + (1-\alpha)(c - y(t)) \quad (5.1)$$

If the sequence  $x(t)$  tends to an equilibrium value  $\bar{x}$ , that is, if the corresponding auto-regressive model is stable, then the output  $y(t)$  tends to an equilibrium value  $y(\infty)$  which equals to set speed in the case of closed-loop prediction. But differs from set speed for open-loop prediction, because, as it is explained in chapter 3, section D, the open-loop prediction produces a bias term which deviates  $y(\infty)$  from set speed.

The closed-loop one-step prediction control equation was :

$$(1-\alpha)(c - y(t)) = y_m(t+1) - y_m(t). \quad (5.2)$$

Rewriting the above equation in terms of impulse responses one gets

$$(1-\alpha)\left(c - \sum_{j=0}^N h_j x(t-j-1)\right) = \sum_{j=0}^N \hat{h}_j x^*(t-j) - \sum_{j=0}^N \hat{h}_j x^*(t-j-1) \quad (5.3)$$

In order to be able to analyze the stability of the system, we have to examine the response of the optimally controlled system to the set point  $c$ , that is, the relationship between  $y(t)$  and  $c(t)$ . This relationship is found in the  $Z$  domain as follows. If the equation (5.3) is transformed to the  $Z$  domain, the equation becomes

$$(1-\alpha)(C(z) - z^{-1} H(z)X(z)) = \hat{H}(z)X(z) - z^{-1} \hat{H}(z)X(z) \quad (5.4)$$

$$(1-\alpha)C(z) = (z^{-1}(1-\alpha)H(z) + (1-z^{-1})\hat{H}(z))X(z) \quad (5.5)$$

$$\frac{X(z)}{C(z)} = \frac{(1-\alpha)}{z^{-1}(1-\alpha)H(z) + (1-z^{-1})\hat{H}(z)} \quad (5.6)$$

Since

$$Y(z) = z^{-1} H(z) X(z), \quad (5.7)$$

then

$$\frac{Y(z)}{C(z)} = \frac{z^{-1} H(z)(1-\alpha)}{z^{-1}(1-\alpha)H(z) + (1-z^{-1})\hat{H}(z)} \quad (5.8)$$

The closed-loop transfer function obtained above can be represented as a block diagram as it is shown in Fig. 5.1.

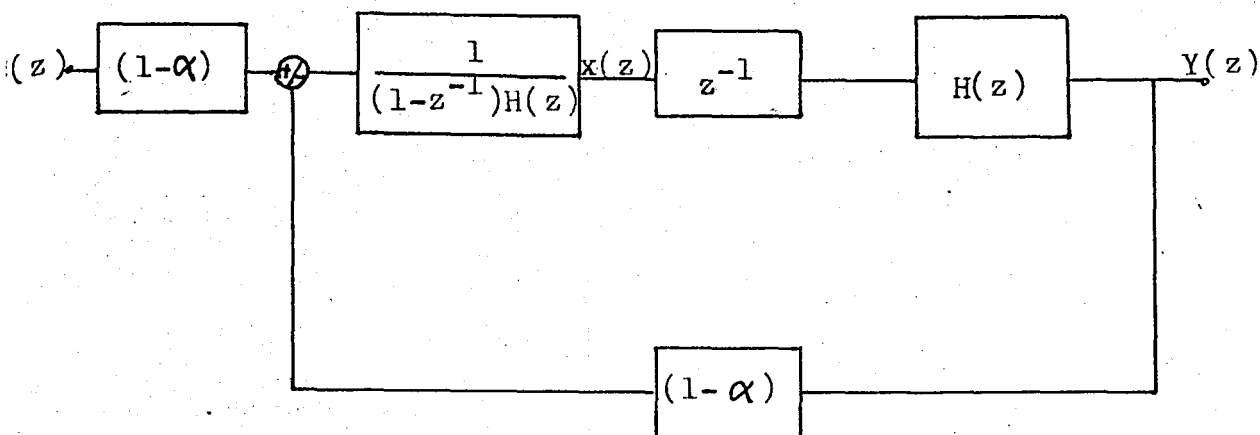


Fig. 5.1 Closed-loop prediction

If the identification of the system impulse response  $\underline{h}^T$  can be considered as perfect, that is,  $H(z) = \hat{H}(z)$ , the closed loop transfer function becomes

$$\frac{X(z)}{C(z)} = \frac{(1 - \alpha)}{(1 - \alpha z^{-1})H(z)} \quad (5.9)$$

and

$$\frac{Y(z)}{C(z)} = \frac{(1 - \alpha)z^{-1}H(z)}{(1 - \alpha z^{-1})H(z)} \quad (5.10)$$

The boundedness condition for the input sequence  $x^*(t)$  is identical to the stability of the auto-regressive model, that is, the polynomial in the denominator of the equation (5.8) which is rewritten in equation (5.11) must have all its roots within the unit circle.

$$z^{-1}(1-\alpha)H(z) + (1-z^{-1})\hat{H}(z) = 0 \quad (5.11)$$

Under the consideration of perfect identification the transfer function of  $Y(z)$  with respect to  $C(z)$  is the first order and identical to the reference trajectory. Since the  $|\alpha|$  is always less than 1, the system is always stable.

We have to consider the case of imperfect identification  $H(z) \neq \hat{H}(z)$ . From the transfer functions (5.6), (5.8) it becomes clear that for the output  $y(t)$  to be convergent and the optimum input sequence to be bounded, it is necessary and sufficient that the denominator of equation (5.8) has all its roots within the unit circle.

In general the exact plant transfer function  $H(z)$  is not known and therefore one can not evaluate the exact expression of the polynomial in equation (5.11). However, if the identification of  $H(z)$  is fairly good, then it is expected that the roots of  $z^{-1}(1-\alpha)H(z) + (1-z^{-1})\hat{H}(z)$  be close to the roots of  $(1-\alpha z^{-1})H(z)$ . Therefore, the stability of the identified model  $\hat{H}(z)$  implies the stability of the controlled system. But when the identification error becomes large so that the discrepancy between  $H(z)$  and  $\hat{H}(z)$  becomes significant, then to determine the stability of the system one should recourse to robustness analysis which involves determining the set of plant polynomials  $H(z)$  for which the above characteristic polynomials have stable roots.

### 1. Robustness of the System

The control is said to be robust if the plant output  $y(t)$

converges to its ultimate desired value  $c$ , under a range of plant and behavior changes caused, for instance, by failure of some of its components or by large parameter changes, etc.

With regard to the closed loop prediction control, the robustness problem is posed in terms of the stability of the input sequence  $x(t)$  and the plant output  $y(t)$ . This is a consequence of the fact that the stability of the closed loop system guarantees the unbiased convergence of the output to the set point. Therefore, as long as the structural changes of the plant, which amount to altering the impulse response  $\underline{h}^T$  from its nominal (identified) model  $\hat{\underline{h}}^T$ , are such that the characteristic polynomial (5.11) has all its roots within the unit circle, the control is robust.

Given the model  $\hat{\underline{h}}^T$ , it is of great interest to find a range for the  $(N+1)$  dimensional vector  $\underline{h}^T$  such that (5.11) is stable. The delimitation of such a subspace of  $R^{N+1}$  requires complex search algorithms, and, unrealistic amounts of computation. But fortunately, in most all practical problems, valuable additional information on the physical properties of the plant is available, the appropriate use of this information reduces substantially the size and dimension of the search space. For instance, if the robustness against identification errors or small perturbations is considered, then

$$h_i = \hat{h}_i + \xi_i \quad i=0, \dots, N \quad (5.12)$$

where  $|\xi_i|$  are small with respect to  $\hat{h}_i$  and their upper bounds can be estimated from the particular identification scheme in operation and also the stability can be tested.

As a simple example, let us consider the case where the mismatch between  $\underline{h}^T$  and  $\hat{\underline{h}}^T$  is a pure gain,  $\underline{h}^T = q\hat{\underline{h}}^T$ . As it is explained, the impulse response is represented by a finite number of elements, then a certain magnitude value of the impulse is accepted as zero. Because of the gain error, the impulse response representing the system will decay this certain value faster than the actual system. The maximum possible mismatch gain is usually larger than unity. Then slowing down the reference trajectory (increasing the  $\alpha$ ) improves the robustness of the system.

## 2. Amplitude Constraint on Input

As it is in this application, the input sequence  $x(t)$  is usually not free of constraints. In general, there are both amplitude and rate constraints imposed by technical and cost considerations.

In this thesis the speed reference input of the thyristor unit is constrained by 10V as a result of 8 bit digital to analog converters output capability which is 10V. The speed reference input of the thyristor unit is 0 to -15V, but the maximum output of the digital to analog converter is 10V which is inverted by an operational amplifier. If the system is forced to reach its maximum rated speed (1400 rpm) from zero speed, in the first few sampling intervals the error term  $\frac{(1-\alpha)}{h_0} (c-y(t))$  is maximum. At these intervals the algorithm in the computer will calculate maximum speed references to be able to reach the set speed as fast as possible, however, no matter how big the input is



calculated, the applied maximum speed reference input is -10V. This causes the system reach the set speed slower.

The above discussion, amplitude constraint does not effect the system stability, but limits the selectable range of  $\alpha$ . The meaning of this limitation in  $\alpha$ , in practical application is that the rate of reference trajectory is also limited. The output of 10 bit analog to digital converter is 782 in decimal system (30E in hex.) when the motor rotating at 1400 rpm (146.6). The resolution of A/D converter is then 1.79 rpm/bit, or 0.18747 rad/sec/bit. The FF in the input of D/A converter produces 10V at the output. From the equation (3.25) the error term is

$$\frac{(1-\alpha)}{h_0} (c-y(t)). \quad (5.13)$$

Let us suppose that the motor is not rotating and no past history is available in the memory. In the first sampling period while calculating  $x(0)$  only the above equation is manipulated. The calculation will be as follows

$$0.18747 \frac{(1-\alpha)}{h_0} (782 - 0) = x(0) = 255. \quad (5.14)$$

Since all calculations are done in rad/sec, the speed of the motor is multiplied by 0.18747 to get the speed in rad/sec. Equation is equaled to 255 to be able to obtain maximum speed reference output from the D/A converter.

From the equation (5.14) minimum  $\alpha$  is found to be 0.96 .

Therefore

$$0.96 \leq \alpha < 1 . \quad (5.15)$$

### B.Experimental Results

The experiments are done for two different time constants of software reference trajectory, which are the maximum allowable  $\alpha$  and the minimum one. Also to observe the system response to parameter variations, an induction motor is coupled to the dc motor to change the moment of inertia of the system.

Fig. 5.2 is the time response of the motor speed for  $\alpha = 0.967$  with the induction motor coupled and without it. In Fig. 5.3 the same process is repeated for  $\alpha = 0.99$ .

As it can be seen from these oscillograms, the change in one of the system parameters, namely the moment of inertia does not effect the performance of the system.

If the output of the system at time  $(t+1)$  is exactly equal to the predicted value, the relation between the time constant and the value of  $\alpha$  can be obtained as below.

The reference trajectory was

$$y_r(t+1) = \alpha y_r(t) + (1-\alpha)c , \quad (5.16)$$

and from equation (1.16) the system equation is

$$\dot{y}_m(t) = -\frac{1}{t_m} y_m(t) + \frac{K_m}{t_m} e_a(t) \quad (5.17)$$

the discrete equivalent of above equation is

$$y_m(t+1) = e^{-\frac{T}{T_m}} y_m(t) + K_m(1 - e^{-\frac{T}{T_m}}) e_a(t). \quad (5.18)$$

Thus

$$\alpha = e^{-\frac{T}{T_m}}, \quad (5.19)$$

therefore, for  $\alpha = 0.99$ ,  $T_m = 0.7959$  sec. and for  $\alpha = 0.967$ ,  $T_m = 0.2384$  sec.

Although the time constant of the step response is not expected to be equal to that determined by the value of  $\alpha$  due to continual updating, it is seen that the time constants of the responses are very close to those values.

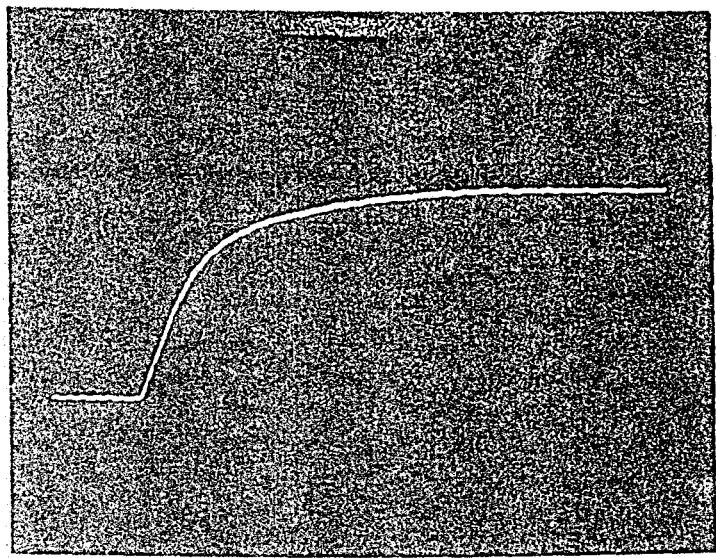
The oscillograms of Fig. 5.4 show the tracking behavior of the system. For these tests, the set speed is changed continuously for 3 seconds and then it is kept constant and finally for the last 3 seconds  $c$  is decreased in a linear fashion. In other words, a time optimal set speed change is applied. As discussed in chapter three, the maximum acceleration that the system is capable of is  $11.27 \text{ rad/sec}^2$ . Starting with an initial speed of 600 rpm, the set speed was therefore changed by 0.86 rpm per sampling interval until a final set speed of 923 rpm was reached. The same procedure was followed for deceleration. It is seen that from the oscillograms of Fig. 5.4 that this reference trajectory is followed very closely. The response for  $\alpha = 0.99$  are not shown because for this value

of  $\alpha$ , the tracking behavior is not very good due to the fact that a change of 0.86 rpm in the set speed can only be followed with a time constant of 0.967. If slower time constants are applied, the tracking error accumulates at the end.

Fig. 5.4.b shows that the tracking performance does not change appreciably due to the change in  $J$ . The slight difference in Fig. 5.4.a and b are due to the fact that the time of acceleration, the time during which set speed was kept constant and the time of deceleration were decided upon by a simple observation of the CRT spot in the horizontal axis.

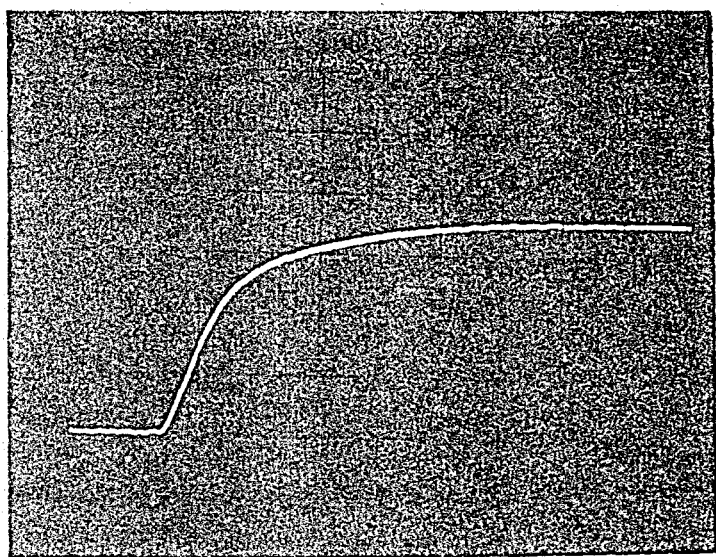
Fig. 5.5.a and b show the responses of the system under loaded conditions. A comparison of these with those of Fig. 5.2.a and b show that the loading does not effect the performance especially for the time varying set speed case.

700 rpm



(a)

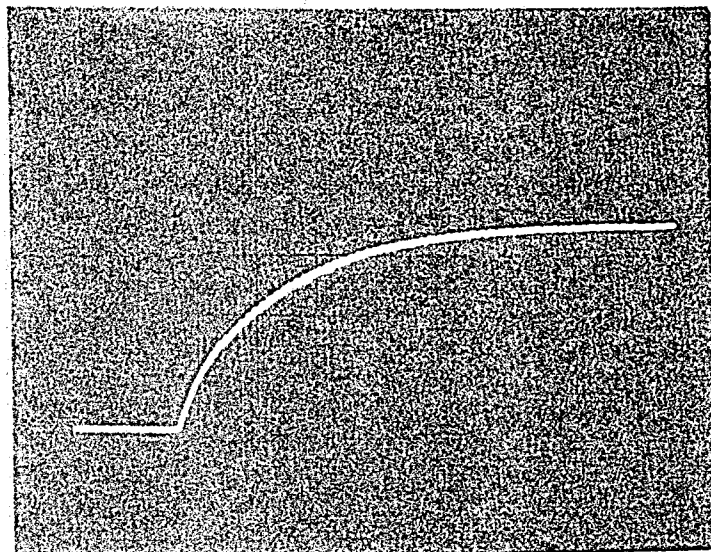
700 rpm



(b)

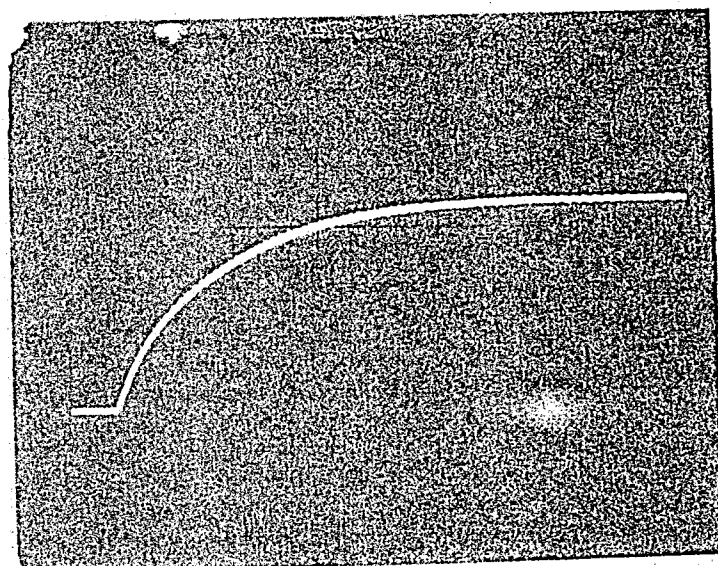
Fig. 5.2 The time response of the motor speed  
 $\alpha = 0.967$  1 div. = 0.2 sec = 200 rpm  
(a) without induction motor  
(b) with induction motor.

700 rpm



(a)

700 rpm



(b)

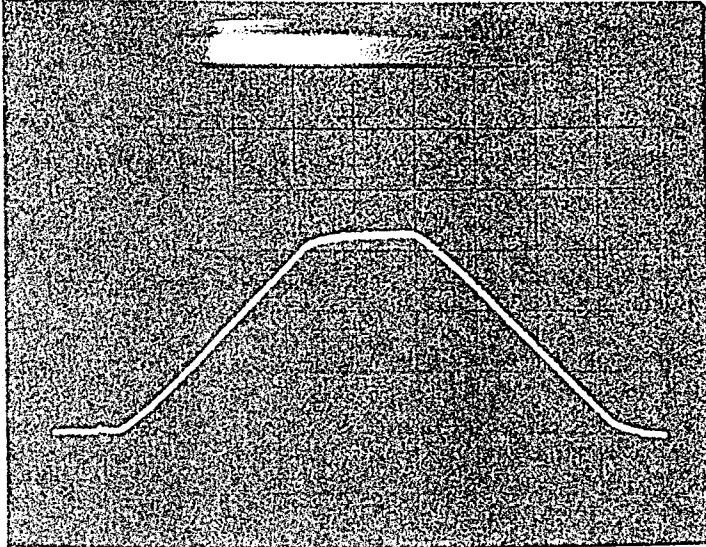
Fig. 5.3 The time response of the motor speed

$\alpha = 0.99$  1 div. = 0.5 sec = 200rpm

(a) without induction motor

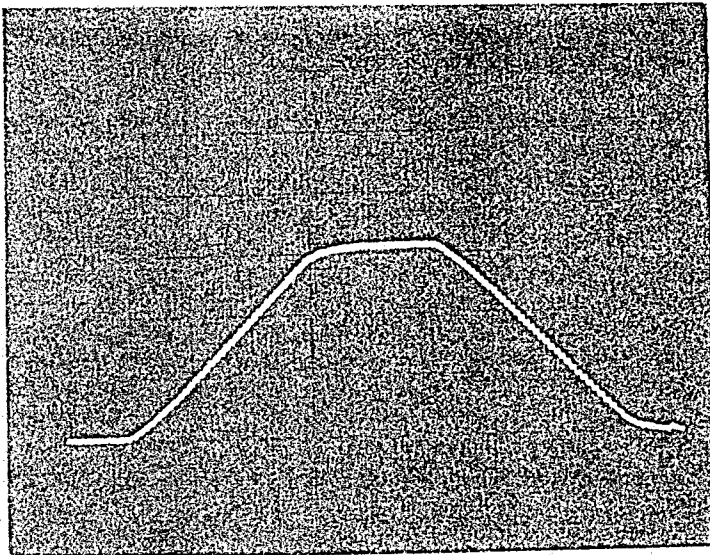
(b) with induction motor.

600 rpm



(a)

600 rpm



(b)

Fig.5.4 The tracking behavior of the motor speed

$\alpha = 0.967$  1 div. = 1 sec = 100 rpm

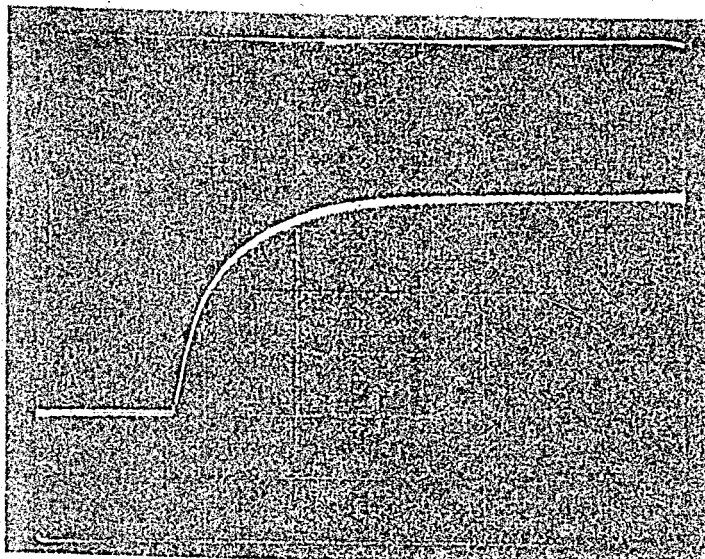
3 sec. acceleration, 2 sec. max. speed and

3 sec. deceleration

(a) without induction motor

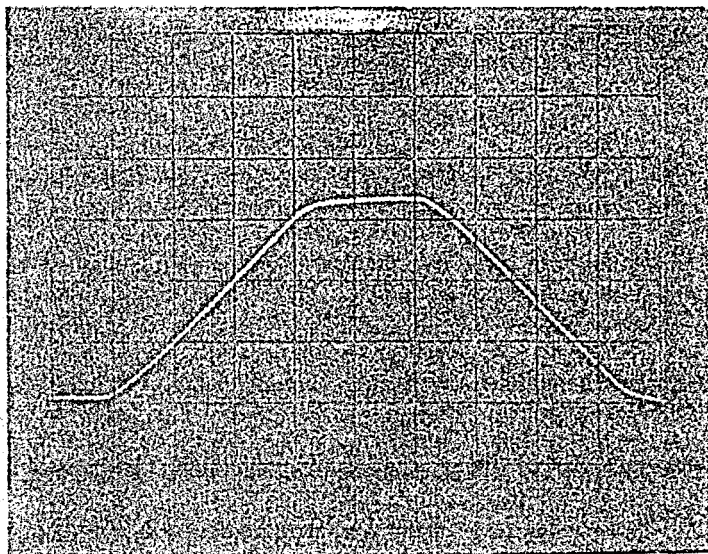
(b) with induction motor.

700 rpm



(a)

600 rpm



(b)

Fig. 5.5 The behavior of the system under load

(a)  $\alpha=0.967$  1 div. = 0.2 sec. = 200 rpm

(b)  $\alpha=0.967$  1 div. = 1 sec. = 100 rpm.



## VI. CONCLUSIONS AND SUGGESTIONS FOR FURTHER WORK

In the thesis, the speed control of a separately excited dc motor is achieved by using Model Algorithmic Control. The starting point of this theory is that the process to be controlled should be relatively slow and the controller must have fast digital computing and memory facilities.

The frequency of microcomputer used in the implementation of the theory is 2.5 MHz, than the controller can be considered as a relatively slow one. As it is explained, to overcome this disadvantage, the coefficients in the control equation is grouped as shown in Fig. 4.3

The coefficients are approximated twice, first because of truncation errors and than because of the error caused by grouping them. In spite of these approximations, it is shown that the steady state error can be considered as zero. Also it is shown that the system is robust, and therefore Model Algorithmic Control is a good candidate for cases in which robust performance is required.

The D/A converter used in the hardware is an 8-bit one and the inverted output of which is -10 V. The speed reference input of the thyristor unit is -15 V. This brings an important constraint in the optimal input sequence. This constraint does

not effect the system stability and robustness, but limits the value of  $\alpha$  , and the time constant of the process output. This is especially important for tracking case, because the tracking performance of the Model Algorithmic Control is better for small software time constants. If a proper D/A converter could be available, the region of selectable  $\alpha$  would have been wider, and the system would have been operated with smaller time constants.

The performance obtained by the work described in the thesis is very promising, warranting a more through theoretical analysis of the Model Algorithmic Control theory as applied to the dc motor speed control. The theoretical analysis presented in this thesis neglects the effects of current control loop. The constraint imposed by the set maximum value of the current and the effects of the P controller of the current loop should be investigated to gain more insight to the design of a Model Algorithmic Controller.

The performance obtained suggest that the application of Model Algorithmic Control to manipulator control could alleviate the problems that arise in such a system due to high degree of coupling between the links and due to variations in the pay load. The Lagrange-Euler approach to formulate the robot arm dynamics result in a set of highly coupled differential equations making its control difficult. However for the application of Model Algorithmic Control theory only an impulse response representation is required and this can be obtained rather easily. The variations in the impulse response due to different arm positions should not effect the arm trajectory as demonstrated in the thesis.

## APPENDIX A

SOFTWARE OF MODEL ALGORITHMIC CONTROL  
FOR CONSTANT SET SPEED

210042	LD HL,4200H	
363C	LD (HL),3CH	;Coefficients of
23	INC HL	control equation
3633	LD (HL),33H	
23	INC HL	
3629	LD (HL),29H	
23	INC HL	
3620	LD (HL),20H	
23	INC HL	
3618	LD (HL),18H	
23	INC HL	
3611	LD (HL),11H	
23	INC HL	
360C	LD (HL),0CH	
23	INC HL	
3609	LD (HL),09H	
23	INC HL	
3606	LD (HL),06H	
23	INC HL	
3604	LD (HL),04H	
23	INC HL	
3603	LD (HL),03H	
23	INC HL	
3602	LD (HL),02H	

23		INC	HL	
3601		LD	(HL),01H	
23		INC	HL	
363C		LD	(HL),3CH	; α
D300	MAIN:	OUT	(00),A	;Apply speed ref.
210040		LD	HL,4000H	input of thyristor
0605		LD	B,05	unit
97		SUB	A	;Calculation of
57		LD	D,A	$b_1 x^{*(t-1)} + \dots +$
86	L1:	ADD	A,(HL)	$b_N x^{*(t-N)}$
D23A30		JP	NC,M1	
14		INC	D	
23	M1:	INC	HL	
10F8		DJNZ	L1	
210042		LD	HL,4200H	
4E		LD	C,(HL)	
5F		LD	E,A	
CD3232		CALL	MULT	
226232		LD	(TEMP1),HL	
210540		LD	HL,4005H	
0605		LD	B,05H	
97		SUB	A	
57		LD	D,A	
86	L2:	ADD	A,(HL)	
D25B30		JP	NC,M2	
14		INC	D	
23	M2:	INC	HL	
10F8		DJNZ	L2	
210142		LD	HL,4201H	
4E		LD	C,(HL)	
5F		LD	E,A	
CD3232		CALL	MULT	
226432		LD	(TEMP2),HL	
210A42		LD	HL,420AH	
0608		LD	B,08H	
97		SUB	A	
57		LD	D,A	
86	L3:	ADD	A,(HL)	

D27530		JP	NC, M3
14		INC	D
23	M3:	INC	HL
10F8		DJNZ	L3
210242		LD	HL, 4202H
4E		LD	C, (HL)
5F		LD	E, A
CD3232		CALL	MULT
226632		LD	(TEMP3), HL
211240		LD	HL, 4012H
0608		LD	B, 08
97		SUB	A
57		LD	D, A
86	L4:	ADD	A, (HL)
D28F30		JP	NC, M4
14		INC	D
23	M4:	INC	HL
10F8		DJNZ	L4
210342		LD	HL, 4203H
4E		LD	C, (HL)
5F		LD	E, A
CD3232		CALL	MULT
226832		LD	(TEMP4), HL
211A40		LD	HL, 401AH
060A		LD	B, 0AH
97		SUB	A
57		LD	D, A
86	L5:	ADD	A, (HL)
D2A930		JP	NC, M5
14		INC	D
23	M5:	INC	HL
10F8		DJNZ	L5
210442		LD	HL, 4204H
4E		LD	C, (HL)
5F		LD	E, A
CD3232		CALL	MULT
226A32		LD	(TEMP5), HL

212440		LD	HL, 4024H
060A		LD	B, 0AH
97		SUB	A
57		LD	D, A
86	L6:	ADD	A, (HL)
D2C330		JP	NC, M6
14		INC	D
23	M6:	INC	HL
10F8		DJNZ	L6
210542		LD	HL, 4205H
4E		LD	C, (HL)
5F		LD	E, A
CD3232		CALL	MULT
226C32		LD	(TEMP6), HL
212E40		LD	HL, 402EH
060A		LD	B, 0AH
97		SUB	A
57		LD	D, A
86	L7:	ADD	A, (HL)
D2C530		JP	NC, M7
14		INC	D
23	M7:	INC	HL
10F8		DJNZ	L7
210642		LD	HL, 4206H
4E		LD	C, (HL)
5F		LD	E, A
CD3232		CALL	MULT
226E32		LD	(TEMP7), HL
213840		LD	HL, 4038H
060D		LD	B, 0DH
97		SUB	A
57		LD	D, A
86	L8:	ADD	A, (HL)
D2C730		JP	NC, M8
14		INC	D
23	M8:	INC	HL
10F8		DJNZ	L8
210742		LD	HL, 4207H

4E		LD	C, (HL)
5F		LD	E, A
CD3232		CALL	MULT
227032		LD	(TEMP8), HL
214540		LD	HL, 4045H
060D		LD	B, 0DH
97		SUB	A
57		LD	D, A
86	L9:	ADD	A, (HL)
D2C930		JP	NC, M9
14		INC	D
23	M9:	INC	HL
10F8		DJNZ	L9
210842		LD	HL, 4208H
4E		LD	C, (HL)
5F		LD	E, A
CD3232		CALL	MULT
227232		LD	(TEMP9)
215240		LD	HL, 4052H
060D		LD	B, 0DH
97		SUB	A
57		LD	D, A
86	LA:	ADD	A, (HL)
D2CB30		JP	NC, MA
14		INC	D
23	MA:	INC	HL
10F8		DJNZ	LA
210942		LD	HL, 4209H
4E		LD	C, (HL)
5F		LD	E, A
CD3232		CALL	MULT
227432		LD	(TEMPA), HL
215F40		LD	HL, 405FH
060F		LD	B, 0FH
97		SUB	A
57		LD	D, A
86	LB:	ADD	A, (HL)

D2CD30		JP	NC,MB
14		INC	D
23	MB:	INC	HL
10F8		DJNZ	LB
210A42		LD	HL,420AH
4E		LD	C,(HL)
5F		LD	E,A
CD3232		CALL	MULT
227632		LD	(TEMPB),HL
216E40		LD	HL,406EH
060F		LD	B,0FH
97		SUB	A
57		LD	D,A
86	LC:	ADD	A,(HL)
D2CF30		JP	NC,MC
14		INC	D
23	MC:	INC	HL
10F8		DJNZ	LC
210B42		LD	HL,420BH
4E		LD	C,(HL)
5F		LD	E,A
CD3232		CALL	MULT
227832		LD	(TEMPC),HL
217C40		LD	HL,407CH
060F		LD	B,0FH
97		SUB	A
57		LD	D,A
86	LD:	ADD	A,(HL)
D2d130		JP	NC,MD
14		INC	D
23	MD:	INC	HL
10F8		DJNZ	LD
210C42		LD	HL,420CH
4E		LD	C,(HL)
5F		LD	E,A
CD3232		CALL	MULT
227A32		LD	(TEMPD),HL



210000	LD	HL,0000	
ED5B6232	LD	DE,(TEMP1)	
19	ADD	HL,DE	
ED5B6432	LD	DE,(TEMP2)	
19	ADD	HL,DE	
ED5B6632	LD	DE,(TEMP3)	
19	ADD	HL,DE	
ED5B6832	LD	DE,(TEMP4)	
19	ADD	HL,DE	
ED5B6A32	LD	DE,(TEMP5)	
19	ADD	HL,DE	
ED5B6C32	LD	DE,(TEMP6)	
19	ADD	HL,DE	
ED5B6E32	LD	DE,(TEMP7)	
19	ADD	HL,DE	
ED5B7032	LD	DE,(TEMP8)	
19	ADD	HL,DE	
ED5B7232	LD	DE,(TEMP9)	
19	ADD	HL,DE	
ED5B7432	LD	DE,(TEMPA)	
19	ADD	HL,DE	
ED5B7632	LD	DE,(TEMPB)	
19	ADD	HL,DE	
ED5B7832	LD	DE,(TEMPC)	
19	ADD	HL,DE	
ED5B7A32	LD	DE,(TEMPCD)	
19	ADD	HL,DE	
226032	LD	(TEMP),HL	
DB00	IN	A,(00)	;Read the actual
5F	LD	E,A	speed
DB01	IN	A,(01)	
E603	AND	03H	
57	LD	D,A	
2A5E32	LD	HL,(SETSPD)	
37	SCF		
3F	CCF		
ED52	SBC	HL,DE	
EB	EX	DE,HL	
210D42	LD	HL,420DH	;Calculate the
4E	LD	C,(HL)	error term

CD4C32		CALL	MULT1	
ED5B6032		LD	DE,(TEMP)	
19		ADD	HL,DE	;Calculate x*(t)
FC		LD	A,H	
32FF3F		LD	(3FFFH),A	
019200		LD	BC,0092H	;Update the past
219040		LD	HL,4090H	history
119140		LD	DE,4091H	
ED5B		LDDR		
CD1B00		CALL	GETKY	
FE21		CP	21H	;SHIFT + ! pressed ?
CA1D32		JP	Z,MODIFY	;Yes
FE49		CP	49H	;I pressed ?
CA2632		JP	Z,INCRS	;Yes
FE44		CP	44H	;D pressed ?
CA2632		JP	Z,DCRS	;Yes
C32C32		JP	IN	
97	MODIFY:	SUB	A	;Clear the speed
DC00		OUT	(00),A	reference input
0691		LD	B,91H	of thyristor unit
21FF3F		LD	HL,3FFFH	
77	LR:	LD	(HL),A	
23		INC	HL	
10FC		DJNZ	LR	
C30060		JP	BRK	
210E03	INCRS:	LD	HL,030EH	;Increase the set
225E32		LD	(SETSPD),HL	speed
C32C32		JP	IN	
218701	DCRS:	LD	HL,0187H	;Decrease the set
225E32		LD	(SETSPD),HL	speed
3AFF3F	IN:	LD	A,(3FFFH)	
C33130		JP	MAIN	
210000	MULT:	LD	HL,0000	;6 bit multiplier
0606		LD	B,06H	with zero initial
CB09	LC2:	RRC	C	value
D23D32		JP	NC,LC1	
19		ADD	HL,DE	
CB13	LC1:	RL	E	

CB12		RL D	
10F4		DJNZ LC2	
0603		LD B,03H	
CB3C	LC3:	SRL H	
CB1D		RR L	
10FA		DJNZ LC3	
C9		RET	
210000	MULT1:	LD HL,0000	;7 bit multiplier
0607		LD B,07H	with zero initial
CB09	LB2:	RRC C	value
D25732		JP NC,LB1	
19		ADD HL,DE	
CB13	LB1:	RL E	
CB12		RL D	
10F4		DJNZ LB2	
C9		RET	

```

SETSPD: DEFW 030EH
TEMP  : DEFW 0000
TEMP1 : DEFW 0000
TEMP2 : DEFW 0000
TEMP3 : DEFW 0000
TEMP4 : DEFW 0000
TEMP5 : DEFW 0000
TEMP6 : DEFW 0000
TEMP7 : DEFW 0000
TEMP8 : DEFW 0000
TEMP9 : DEFW 0000
TEMPA : DEFW 0000
TEMPB : DEFW 0000
TEMPC : DEFW 0000
TEMPD : DEFW 0000
BRK   : EQU 6000H
GETKY : EQU 001BH
      END

```

## APPENDIX B

## SOFTWARE OF MODEL ALGORITHMIC CONTROL

## FOR TIME VARYING SET SPEED

The difference between the software of constant set speed and time varying set speed is in the program sections labelled by INCRS and DCRS in Appendix A. If we change the below program with the programs labelled INCRS and DCRS in the software of constant set speed, the system runs as a tracking type model algorithmic control.

.	.		
.	.		
.	.		
C30060		JP	BRK
211000	INCRS:	LD	HL,0010H ;The increase at
ED5BBE32		LD	DE,(SPD) the set speed
19		ADD	HL,DE
22BE32		LD	(SPD),HL
37		SCF	
3F		CCF	
11C061		LD	DE,61C0H
ED52		SBC	HL,DE

F23332		JP	P, PR	;If reached the max.
C33A32		JP	NOR	set speed ?
EB	PR:	EX	DE, HL	
22BE32		LD	(SPD), HL	
C34932		JP	LL	
2ABE32	NOR:	LD	HL, (SPD)	
CB65		BIT	4, L	
CA4532		JP	Z, XX	
C34932		JP	LL	
112000	XX:	LD	DE, 0020H	
19		ADD	HL, DE	
0605	LL:	LD	B, 05H	
37	YY:	SCF		
3F		CCF		
CB1C		RR	H	
CB1D		RR	L	
10F8		DJNZ	YY	
22BC32		LD	(SETSPD), HL	
C38A32		JP	IN	
111000	DCRS:	LD	DE, 0010H	;The decrease at the
2ABE32		LD	HL, (SPD)	set speed
37		SCF		
3F		CCF		
EB52		SBC	HL, DE	
22BE32		LD	(SPD), HL	
37		SCF		
3F		CCF		
110000		LD	DE, 0000	
ED52		SBC	HL, DE	
FA7332		JP	M, NN	;If reached zero
C37A32		JP	OK	set speed ?
EB	NN:	EX	DE, HL	
22BE32		LD	(SPD), HL	
C37D32		JP	OO	
2ABE32	OK:	LD	HL, (SPD)	
0605	OO:	LD	B, 05H	
37	MM:	SCF		
3F		CCF		

CB1C		RR	H
CB1D		RR	L
10F8		DJNZ	MM
22BC32		LD	(SETSPD),HL
3AFF3F	IN:	LD	A,(3FFH)
C33130		JP	MAIN
210000	MULT:	LD	HL,0000
.		.	.
.		.	.
.		.	.

## BIBLIOGRAPHY

1. J. Richalet, A. Rault, J. L. Testud and J. Papon, "Model Predictive Heuristic Control : Application to Industrial Processes" , Automatica, Vol. 14, pp. 413-428, 1978.
2. R. Rouhani and R. K. Mehra, "Model Algorithmic Control: Basic Theoretical Properties," Automatica, Vol.18, pp. 401-414.
3. Kusko, Alexander. Solid-State DC Motor Drives, New York, The MIT Press, 1969.
4. Sen, Paresh C. Thyristor DC Drives, New York, Wiley-Interscience, 1980.
5. Katz, Poul. Digital Control Using Microprocessors, New Jersey, Prentice-Hall International Inc.,1981.
6. Leventhal, Lance. Z-80 Assembly Language Programming, Berkeley, California, 1979.